JLB

RI 7963

Bureau of Mines Report of Investigations/1974

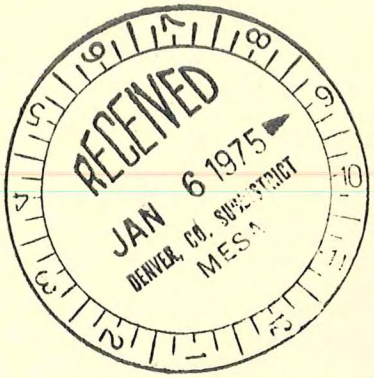

Infrared Spectra of Compounds of Importance in Lead Sulfide Flotation

UNITED STATES DEPARTMENT OF THE INTERIOR

Report of Investigations 7963

Infrared Spectra of Compounds of Importance in Lead Sulfide Flotation

By Roy L. Wilfong and Edwin E. Maust, Jr.
College Park Metallurgy Research Center, College Park, Md.

UNITED STATES DEPARTMENT OF THE INTERIOR
Rogers C. B. Morton, Secretary

Jack W. Carlson, Assistant Secretary–Energy and Minerals

BUREAU OF MINES
Thomas V. Falkie, Director

This publication has been cataloged as follows:

Wilfong, Roy L

Infrared spectra of compounds of importance in lead sulfide flotation, by Roy L. Wilfong and Edwin E. Maust, Jr. [Washington] U.S. Bureau of Mines [1974]

65 p. illus., tables. (U.S. Bureau of Mines. Report of investigations 7963)

Includes bibliography.

1. Lead sulphide. I. Maust, Edwin E., jt. auth. II. U.S. Bureau of Mines. III. Title. IV. Title: Lead sulfide flotation. (Series)

TN23.U7 no. 7963 622.06173

U.S. Dept. of the Int. Library

CONTENTS

ILLUSTRATIONS

TABLES

INFRARED SPECTRA OF COMPOUNDS OF IMPORTANCE IN LEAD SULFIDE FLOTATION

by

Roy L. Wilfong[1] and Edwin E. Maust, Jr.[2]

ABSTRACT

Infrared reference spectra are presented of compounds of importance in lead sulfide flotation research. Included are the spectra of several short chain alkyl xanthates of lead and zinc, the corresponding dixanthogen compounds, and the common oxidation products of lead sulfide and their sodium analogs. The spectra of several frequently used industrial flotation reagent xanthates are also presented.

A thorough, well-documented discussion is given of the various corrections made to correct the as recorded absorption band data to near absolute values.

INTRODUCTION

The ever-increasing demand for mineral commodities requires improved technology to permit the continued mining and treatment of lower and lower grade ores. The sulfide ores are commonly beneficiated through froth flotation. Of central importance in this recovery and separation technique is the chemisorption of reagents which selectively render the surfaces of the sulfide mineral particles hydrophobic. A better understanding of this chemisorption phenomena and the mechanisms that control it is essential if improvements and further development to this ore recovery process are to be realized. While seeking this better understanding, a reservoir of infrared spectra of compounds considered of importance in sulfide flotation research has been prepared and is presented in this paper.

The use and importance of infrared spectroscopy has increased severalfold in recent years, paralleling the increasing availability of relatively inexpensive infrared instrumentation. It was chosen as one of the instrumental tools in the Bureau of Mines varied investigations into flotation adsorption phenomena because of its wide general acceptance for identification of both organic and inorganic substances and its capability of analyzing extremely small samples. Further, it offered several technique options for analyzing

[1]Research chemist.
[2]Supervisory chemical engineer.

samples in various forms. The KBr pellet and Nujol mull direct transmission methods are widely used for powdered solid materials, reflection techniques for bulk materials and surface films, and liquid transmission techniques for both pure liquids in bulk form and soluble liquids and solids in solution.

The KBr pellet technique was chosen to obtain our reference spectra of solid substances. This choice was based on several factors: (1) Reflectance spectra are frequently more difficult to obtain and of lower intensity; (2) the Nujol mulls presents "nuisance" absorption bands with which one must contend with that technique; (3) KBr has excellent transmission properties with no interfering absorption bands over an unusually wide spectral range; and (4) probably most important, the KBr pellet technique was found to give very good resolution.

Numerous investigations into sulfide flotation phenomena and of flotation reagents have been based on infrared spectroscopy. Leja, Little, and Poling (8)[3] studied oxidized and sulfidized copper substrates and evaporated lead sulfide, galena, and lead substrates. Allison, Goold, Nicol, and Granville (2) studied the reaction between sulfide minerals and aqueous xanthate solution. Coleman and Powell (3) investigated the xanthate-galena system as did Allison and Finkelstein (1) and Greenler (6). Goold and Finkelstein (5) studied the potassium alkyl xanthate and alkyl trimethyl ammonium bromide mixed collector system. Coleman, Powell, and Cochran (4) and Yamasaki and Usui (19) investigated xanthate-zinc sulfide systems. Pearson and Stasiak (13) obtained spectral data on several xanthates, oxyxanthates, and dixanthates. Several studies (7, 9, 10, 16, 18) have also been made in efforts to make and clarify band assignments.

Each of the above investigators, plus many other workers, have presented spectral data in one form or another for flotation related compounds. However, in spite of this relatively large literature storehouse, there still exists a scarcity of good reference spectra. The discrepancies in the literature spectra are many. A major shortcoming is that the majority are limited in the spectral range covered, the spectra frequently not covering the complete range of interest. Some show poor resolution, the particular method or instrument that was used apparently having been incapable of producing better results. Quite often, the purity of the sample material that produced the spectrum is of a questionable nature. Furthermore, the spectra exist in a variety of shapes and sizes with several different combinations of ordinate and abscissa units making intercomparing a most time-consuming, difficult task. Also, frequently, all compounds of interest are not included.

Upon encountering these shortcomings in the literature, our own reference spectra were compiled. These were prepared and compiled with the goal of eliminating as many of the above discrepancies as possible. They are presented here to give a single, compact source of good reference spectra of those compounds of principal interest in sulfide flotation research.

---

[3]Underlined numbers in parentheses refer to items in the list of references at the end of this report.

COMPOUNDS OF INTEREST

The reference spectra presented here are of those compounds considered of principal interest in lead sulfide ore flotation. The short alkyl chain potassium xanthates are presented in view of their role as the initial surface contacting species. The lead xanthates are given because they are known adsorbed surface reaction products. The dixanthogens are presented as known xanthate oxidation products and because of the controversy among researchers as to the true role that oxidation and the dixanthogens play in the PbS flotation process. The spectra of the zinc xanthates and cuprous ethyl xanthate are given for comparison with those of the lead xanthates and to serve as an aid in interpretation of the lead xanthate spectra and possibly in attempted band assignments. The several homologues of each type compound may also be found useful in this latter respect.

The common oxidation products, lead sulfate, lead thiosulfate, and lead sulfite are included because they are believed to be involved in xanthate adsorption on lead sulfide (6, 8). Lead carbonate has been included since it too may possibly be a participant in such xanthation reactions (6). The spectra of the industrially used commercial xanthates are of ready interest for comparative purposes.

EXPERIMENTAL

Materials

Reagent-grade potassium ethyl xanthate was twice dissolved in acetone and precipitated with diethyl ether and, after storage, ether washed prior to use. All other potassium xanthates were prepared by first preparing the corresponding alcoholate from reagent-grade alcohol and KOH and then reacting with A.C.S. certified carbon disulfide. Specifically, in each preparation 0.21 mole of alcohol was added to 0.20 mole of powdered KOH and the reaction mixture stirred for approximately 1 hour while cooling at room temperature in a water bath. Then 0.68 mole CS_2 was added very slowly with continued stirring and the reaction mixture was allowed to stand for over 15 hours. The obtained xanthate was then washed 5 times with ether by adding the ether, stirring the resulting mixture, centrifuging it, and then decanting the wash ether. All traces of a reddish liquid byproduct that formed in varying small amounts were extremely difficult to remove. Final drying of the ether-washed material was achieved by vacuum-pumping for 1 hour or longer.

All lead xanthates were prepared by reacting the above potassium xanthates with reagent-grade lead nitrate. In each case, 50 cu cm of 0.02 molar potassium xanthate solution was added to 50 cu cm of 0.01 molar lead nitrate solution, the reacting mixture stirred for 10 minutes, then it was centrifuged, and the reaction solution decanted. The collected lead xanthate precipitate was washed 5 times with distilled water by adding the water, stirring the resulting mixture, centrifuging it, decanting the wash liquid, and then repeating this procedure. Following washing, the precipitates were vacuum-pumped for 4 hours or more to dry.

All zinc xanthates were prepared by reacting the above potassium xanthates with reagent-grade zinc sulfate. Past experience indicated the need for increased solution concentrations above those used for the preparation of the lead xanthates. Five cu cm of 0.2 molar potassium xanthate solution was added to 5 cu cm of 0.1 molar zinc sulfate solution and the reacting mixture was stirred for 10 minutes, was centrifuged, and then the reaction solution was decanted off. The collected zinc xanthate precipitate was then washed and dried by the above procedure used for the lead xanthates.

Cuprous ethyl xanthate was prepared in a similar manner to that used for lead ethyl xanthate except reagent-grade cupric sulfate was used instead of the nitrate. Also, in addition to washing the prepared material with distilled water, it was further washed three times with diethyl ether to remove any dixanthogen that might be present. The washed material was dried under vacuum.

The dixanthogens were each prepared by very slowly adding 2 grams of the above corresponding potassium xanthate powder to 10 cu cm of reagent-grade 30 percent H_2O_2 solution while stirring and cooling at room temperature in a water bath. Following addition of the powder, the mixture was allowed to stand for 1 hour. Then it was centrifuged, the H_2O_2 solution was decanted, and the dixanthogen liquid was washed five times with distilled water by the procedure used for the lead and zinc xanthates. The ethyl dixanthogen was vacuum-pumped for 2 hours to dry. All others were vacuum-pumped for over 4 hours.

The lead thiosulfate was prepared from reagent-grade sodium thiosulfate and lead acetate by adding 100 cu cm of 0.1 molar sodium thiosulfate to 100 cu cm of 0.1 molar lead acetate. The precipitated lead thiosulfate was washed five times with distilled water, air-dried overnight, and further dried by vacuum pumping. The lead sulfite was prepared from reagent-grade sodium sulfite and lead nitrate using the same quantities and concentrations of reagents as those used for the preparation of the lead thiosulfate and washing and drying in like manner. The lead sulfate, lead carbonates, sodium thiosulfate, and sodium sulfite were commercial reagent-grade materials and were used without further purification. The industrial xanthates sodium isopropyl and potassium hexyl were Dow Chemical Company's DOW Z-11[4] [5] and DOW Z-10, respectively. The industrial xanthates sodium isobutyl and potassium amyl were American Cyanamid Company's AERO XAnthate 317[6] and AERO Xanthate 350, respectively. All industrial xanthates were used as received.

Emission spectrographic analysis of the lead sulfate and nonbasic lead carbonate showed only 0.0001-0.001 percent Ag, 0.003-0.03 percent Bi, 0.00003-0.0003 percent Cu, and 0.0003-0.003 percent Fe for the sulfate, and 0.01-0.1 percent Bi, 0.001-0.01 percent Ca, 0.00003-0.0003 percent Cu, 0.0003-0.003 percent Fe, 0.0003-0.003 percent Mn, and 0.01-0.1 percent Na for the carbonate as detectable impurities.

---

[4]The Dow Chemical Company, Midland, Mich.

[5]References to trade names and specific models of equipment are made for identification only and does not imply endorsement by the Bureau of Mines.

[6]American Cyanamid Company, Wayne, N.J.

Distilled, deionized water was used throughout for the preparation of solutions and for all washings.

Instrumentation and Technique

A Perkin-Elmer Model 225 double-beam optical-null grating infrared spectrophotometer was used for all measurements. The solid samples were run using the standard KBr pellet technique. Sample concentrations were 3 to 5 parts per thousand in a 175 mg pellet. The dixanthogen liquids were run as capillary films pressed between two 175 mg KBr pellets. All spectra were obtained with the spectrometer in the double beam mode and using pure KBr as reference. The instrument settings were slit program, 5; gain, 0.50 to 1.40; pen traverse time, 10 seconds; response, 1; scanning speed, fast-1; and suppression, 4.

ACCURACY OF SPECTRAL DATA

Although routine compound identification is frequently based more on the shape, presence, or absence of particular bands in the spectrum than on their absolute position, it is sometimes necessary to have data for band positions on an absolute basis. Moreover, since the spectra reported herein are intended to be of reference quality, an analysis of the accuracy of the data and how it can be corrected as necessary is essential. Accordingly, we provide in this section a discussion of the errors associated with the spectra being reported. Since major emphasis is placed on the recorded charts, the question of accuracy becomes primarily one of calibrating the chart paper and instrument for the particular conditions under which the spectra were run. The spectrum of polystyrene and selected bands from the spectra of water vapor, HCl, and carbon dioxide provided the most convenient basis for this.

A careful check of the instrument and data uncovered one source of consistent error that was not recognized until most of the spectral data had been accumulated. With the chart drum stationary, it was found that the pen did not trace exactly a line of constant wave number as ruled on the chart. In moving across the chart from a position of 90 percent transmittance to one of 5 percent transmittance, the pen traced a line which was apparently (that is, relative to a constant wave number gridline on the printed chart) displaced toward lower wave numbers but not in a linear fashion. Repeating the trace at other drum positions (that is, at other positions on the chart), it was found that the magnitude of the displacement varied from one position to the other. Since the gridlines printed on the as-received charts are used to determine band positions, an error would arise from this source independent of any others. The origin of this particular error is believed to be a combination of misalinement of the pen carriage relative to the axis of the chart drum, and small inaccuracies in the linearity or alinement of the gridlines on the printed charts as received. In any case, a procedure was developed to correct for this error, hereinafter designated "misalinement error" for simplicity.

With a chart mounted on the drum and the instrument set up as usual for running a spectrum, and with the drum not moving, the pen was caused to move

a full scale (approximately 90 percent transmittance to 10 percent transmittance) and back by closing and opening the shutter in the sample beam. This was repeated at each of several drum (chart) positions spaced over the whole range of the chart. The chart was then removed and laid out flat. Using a desk-top magnifying glass with builtin micrometer scale (1 division = 0.005 inch), the change in the position of a trace relative to its position at 90 percent transmittance was determined at intervals of 10 percent transmittance. Seven traces were so measured. The precision of each individual measurement was ±0.1 division, that is, ±0.0005 inch. By a complicated procedure which need not be described here, these 56 values were fitted analytically, as a function of both wave number and transmittance. The resulting equation follows:

$$\delta_1 = A + BT + CT^2 + DT^3, \qquad (1)$$

where $A = 0.369700 + 1.114048 \times 10^{-3} \nu$,

$B = 1.2124588 \times 10^{-2} - 7.1660643 \times 10^{-6} \nu$,

$C = 0.79729666 \times 10^{-3} - 4.4194143 \times 10^{-9} \nu$,

$D = 7.86912212 \times 10^{-6} - 5.943826567 \times 10^{-10} \nu$,

and T is percent transmittance, ν is wave number, and δ_1 is the apparent displacement of a constant wave number trace on the chart relative to its position at 90 percent transmittance, in units of micrometer scale divisions (0.005 inch). The coefficients in equation (1) are forced such that δ_1 is identically zero at T = 90, irrespective of wave number. The experimental values of δ from which this equation was derived are reproduced with an average deviation of ±0.27 divisions and an estimated standard deviation of ±0.35 divisions.

Because the charts change wave number scale at 2,000 cm^{-1}, the error in wave number which corresponds to the trace displacement given by equation (1) is different at higher wave number than at lower wave numbers. Over the range 4,000 to 2,000 cm^{-1}, the wave number scale is 100 cm^{-1} per cm of chart. For this range of wave numbers, then, the correction for misalinement error is 1,270 δ_1 wave numbers. Over the 2,000 to 200 cm^{-1} range the wave number scale is uniformly 40 cm^{-1} per cm of chart, giving a misalinement correction of 0.508 δ_1 wave numbers for this range. In all cases, the misalinement correction must be added to the observed chart reading.

Figure 1 shows the corrections for misalinement obtained from equation (1) and the appropriate factor (1.27 or 0.508). If the grid lines printed on the chart paper were truly straight and parallel lines and if the pen carriage were exactly straight, a small misalinement of either the grid relative to the indexing edge of the chart paper or the pen carriage relative to the axis of the drum would be expected to give a linearly varying trace displacement and one that is independent of wave number. Thus, the trace displacements actually observed imply that the gridlines are not truly straight and their straightness and/or perpendicularity to the indexing edge of the chart paper varies from one end of the chart to the other. Whatever the precise source of the

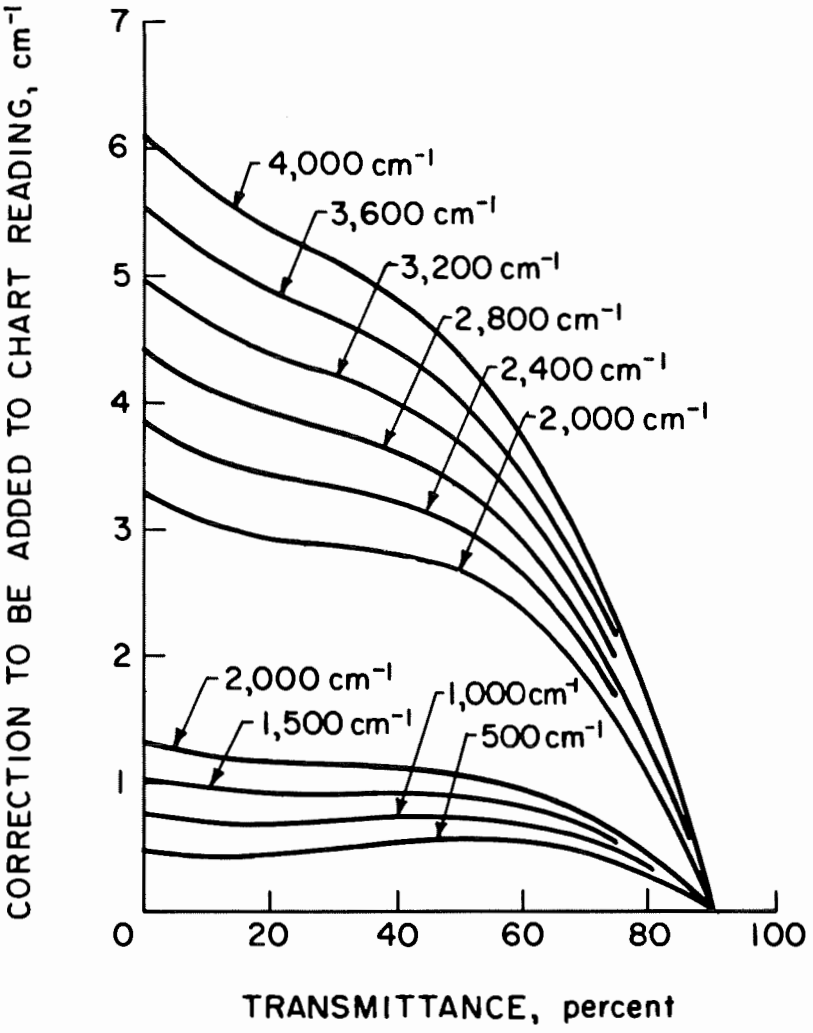

FIGURE 1. - Smoothed corrections for misalinement error.

error, its nature is such that correction for it must be made before, and independent of, any other corrections that might be necessary.

Given any point on the chart, for example, a band position, at a particular wave number and percent transmittance, the correction (1.27 δ or 0.508 δ, depending on the particular wave number) calculated using the above relationships is the wave number equivalent of the amount by which the chart trace would be displaced if the pen were caused to move from that point to the 90 percent transmittance line, without moving the chart. As such, this correction essentially reduces all data to a common baseline at 90 percent transmittance. Any other baseline, for example, 50 percent transmittance, could have been used, and the results would have been similar, the only difference being that corrections for points lying at higher transmittances would have been negative instead of positive. The 90 percent T baseline is more convenient because few, if any, points of experimental interest are likely to occur at higher transmittances; hence, the corrections are almost all positive and mistakes with algebraic signs are reduced.

Percent transmittance has here been used simply as a convenient chart position coordinate. This use does not in any way alter the usual significance of transmittance as a measure of absorption band intensity in interpreting or discussing spectra.

The misalinement error considered here concerns the linearity of gridlines on the chart. The question of how accurately the gridlines are spaced along the 90 percent T baseline is yet to be considered and will be taken up immediately.

Calibration of the 90 percent T baseline on an absolute wave number basis is most convenient to carry out in a two-step procedure. First, corrected chart readings will be related to the wave number dial readings on the instrument. Then, the absolute calibration of the wave number dials will be established. There are two reasons for this seemingly circuitous procedure, both of them based on the fact that there are a limited number of points available for an absolute calibration. The increased resolution obtainable with the wave number dials facilitates calibration of them. The calibration band positions are given in the literature to greater accuracy than the chart can be read. Secondly, one can obtain as many points as desired in relating chart readings to dial readings, irrespective of the number of points available for absolute calibration.

Establishing the relationship between chart and dial readings is complicated by the fact that the relationship changes discontinuously at each of the automatic range changes of the instrument. Table 1 lists the dial readings at the start and end of each range scan. They are quite reproducible. Although the chart drum is stationary while the dials are being reset during the range changes, at the end of this resetting process there is sometimes an abrupt, but small, motion of the drum when the clutch mechanism picks up with the scan of the next range. This normally amounts to about one wave number at the 2,000 and 1,000 cm^{-1} range changes. Thus for example, at the 2,000 cm^{-1} changeover, 1.7 wave numbers are "lost," about half of which is regained by the motion of the drum when the clutch mechanism starts the scan of the next range.

TABLE 1. - Wave number dial readings at the start and end of each range when scanning continuously with automatic range changes

	4,000 to 2,000 cm^{-1}		2,000 to 1,000 cm^{-1}		1,000 to 450 cm^{-1}		450 to 200 cm^{-1}	
	Start[1]	End	Start	End	Start	End	Start	End[2]
Trial:								
1.....	4,000.0	2,000.0	1,998.3	1,000.1	999.38	450.03	449.64	192.25
2.....	4,000.0	2,000.0	1,998.3	-	999.31	450.03	449.66	192.65
3.....	4,000.0	2,000.0	1,998.3	1,000.2	999.35	450.03	449.62	193.62
4.....	4,000.0	2,000.0	1,998.2	1,000.2	999.40	-	449.60	192.0
Average..	4,000.0	2,000.0	1,998.3	1,000.2	999.36	450.03	449.63	-

[1] Forced, as a result of always starting scan with dials set at 4,000.0 cm^{-1}.
[2] Variable in mode of operation used and not necessarily set at 200.0 cm^{-1}.

In deriving the relationship between chart and dial readings, it is assumed that only two basic factors need to be taken into account: (1) expansion or contraction of the chart paper between the time it was printed (by the manufacturer) and the time it was used and (2) inaccuracies in the spacing of the ruled gridlines on the chart. The first, which will be called a shrinkage correction, is assumed to be a uniform expansion or contraction of the chart such that the correction (distancewise) varies linearly over each range. The recorded spectra usually exhibit artifacts at the range changes, probably because of small inaccuracies in resetting the constant-energy slits between ranges, and these can be conveniently used to obtain the shrinkage

corrections. The second factor listed above is obtained simply by taking a sufficient number of observation to construct a curve of chart readings (corrected for misalinement and shrinkage) versus corresponding dial readings. For simplicity, it will be called a grid correction.

In starting a run to record a spectrum, after the chart paper is mounted on the drum and the instrument adjustments made, the wave number dial is set at 4,000.0 cm^{-1} and the chart drum is adjusted and locked into the drive mechanism at that position where the pen is precisely on the 4,000 cm^{-1} gridline of the chart. The position of the pen, transmittancewise, is whatever the sample spectrum dictates. This value is usually not exactly 90 percent transmittance and, hence, must be corrected to the 90 percent T baseline, just as all other chart data. Thus, the corrected chart reading at the start of a run is usually somewhat higher than 4,000.0 cm^{-1} by an amount that depends upon the transmittance level prevailing when the initial chart positioning was carried out. After this initial setting by the operator, the entire spectrum is scanned without human intervention. Hence, the reproducibility and errors associated with range changes are always as indicated in table 1 insofar as dial readings are concerned and can be determined directly from the charts for the chart readings required, the latter corrected for misalinement in accordance with the transmittance at which the artifact in the chart trace occurs.

For each chart, the shrinkage corrections were estimated as follows: After correcting all chart values to the 90 percent T baseline, the corrected values at 4,000 cm^{-1} and each range change were used to derive (least squares) a straight line representing the first estimate of the relationship between chart readings and dial readings. Due account was taken of the discontinuity in dial reading and the jump in chart reading occurring at each range change. The segments of this line corresponding to each span were then adjusted individually by trial and error until the best fit of the range change data was obtained, the adjustments being made in such a way that the average of the two chart readings at each range change remained constant. (Note that this constraint couples the adjustment of one span to the adjustment of adjacent spans.) These lines were then used to interpolate for dial readings corresponding to intermediate chart readings for each span, rather than formulating a shrinkage correction directly. The entire calculation was programmed for digital computation on a time sharing teletype terminal so that the trial and error adjustments could be iterated until changes in the fit became insignificant. Typically, the results of this calculation indicate a paper shrinkage of 1-2 $\times 10^{-3}$ cm/cm, with variations from chart to chart that are large enough to necessitate correction of each chart individually. [Note that chart shrinkage manifests itself as a departure from unity for the slope of chart reading versus dial reading. For the 4,000 cm^{-1} span, this slope is typically 1.002. When intermediate chart readings are interpolated, this slope is effectively multiplied by a number of the order of 2,000 so that a difference of 0.0005 in the slope (that is, a difference of 5×10^{-4} in shrinkage) shows up as a difference of 1.0 wave number in the interpolated value.] In terms of wave numbers, the derived shrinkage corrections vary from zero to a maximum of 4 cm^{-1} and are usually positive, which is to say that the spacing between gridlines on the charts at the range changes is generally less than that required for perfect agreement between chart and dial.

The remaining issue in relating chart readings to dial readings, that is, the grid correction, can now be addressed. This correction was derived by replacing the pen in the instrument with a 36-gage wire pointer and, using a magnifying glass, determining the dial readings corresponding to various gridlines on the chart during a very slow scan over the entire range of the instrument. The chart was initially alined on the 4,000 cm^{-1} line, just as if a spectrum were to be run. During the scan, the pointer was maintained at the 90 percent transmittance level by opening or closing the sample compartment shutter, thus eliminating any complications arising from misalinement error. Chart readings, including values at the range changes, were written down and this data was processed (using the computer program) to obtain shrinkage-corrected values, like a conventional spectrum. Two independent runs were made on different charts. The difference between the shrinkage-corrected chart readings and the corresponding dial readings determined during each scan were fitted empirically to obtain analytic expressions for the grid corrections for each range. The actual data is too voluminous to present in its entirety. The derived equations for the smoothed grid corrections are

200 to 450 cm^{-1}:

$$\delta_2 = 0.1939064 - 3.057324 \times 10^{-4} \nu, \tag{2}$$

450 to 1,000 cm^{-1}:

$$\delta_2 = 1.1784182 - 3.6918272 \times 10^{-3} \nu + 2.6628686 \times 10^{-6} \nu^2, \tag{3}$$

1,000 to 2,000 cm^{-1}:

$$\delta_2 = 3.2668645 - 4.6751856 \times 10^{-3} \nu + 1.5766271 \times 10^{-6} \nu^2, \tag{4}$$

2,000 to 4,000 cm^{-1}:

$$\begin{aligned}\delta_2 = {} & 218.11555 - 0.38113262 \nu + 2.629423 \times 10^{-4} \nu^2 \\ & -8.9542453 \times 10^{-8} \nu^3 + 1.5060747 \times 10^{-11} \nu^4 \\ & -1.0014675 \times 10^{-15} \nu^5.\end{aligned} \tag{5}$$

The corrections given by these equations vary only between the limits -0.2 to + 0.2 cm^{-1} and are to be algebraically added to chart readings already corrected for misalinement and shrinkage.

These corrections were incorporated into the aforementioned computer program and the two sets of data obtained using the wire pointer were reprocessed, the idea being that this precision data should be a good test of how well chart readings can be corrected to yield dial readings. The results are shown in figure 2. Statistically, the difference between corrected chart values and dial readings is not significantly different from zero at the 99 percent confidence level for either set of data. The 140 points in the combined data set are almost equally divided between the two ranges 4,000 to 2,000 cm^{-1} and 2,000 to 200 cm^{-1} and the estimated standard deviation from zero is 0.3 for the former and 0.2 for the latter. The 95 percent confidence band is thus ± 0.6 cm^{-1} for the 4,000 to 2,000 cm^{-1} range and ± 0.4 cm^{-1} for the other, as

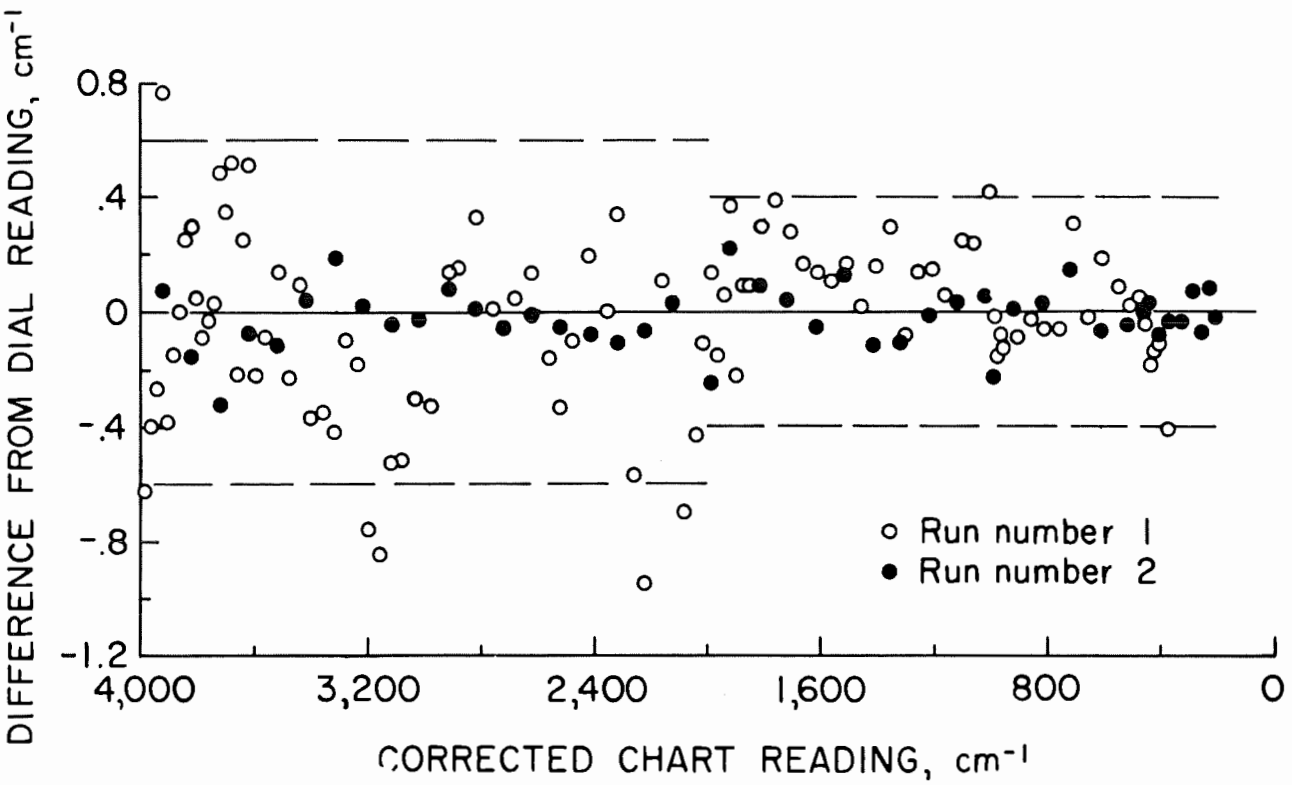

FIGURE 2. - Difference of corrected chart readings from dial readings.

shown on the graph. This is consistent with the slightly poorer readability obtainable on the 4,000 to 2,000 cm^{-1} range of the charts. Of course, these statistics are not typical of what is to be expected in general; they are indicative only of the internal consistency of the shrinkage and grid correction.

Although polystyrene absorption bands are frequently used for calibration purposes in the spectral range of interest here, these bands were found to be too broad to provide a good calibration. Accordingly, H_2O, HCl, NH_3, and CO_2 vapor bands were used, since they are much sharper and in general more accurately known than polystyrene bands. The basic calibration data is given in table 2 and shown graphically in figure 3. Straight lines were fitted to the points, with the exception of the 450 to 200 cm^{-1} range. The data for these water bands was considered less reliable and it was felt that the best procedure was to assume a constant value for the correction over the whole range, equal in magnitude to the average of the seven points obtained (0.54). For the other three ranges, the equations resulting from the fitting procedure follow:

4,000 to 2,000 cm^{-1}:

$$\delta_3 = 1.2233018 - 4.7818406 \times 10^{-4} \nu, \qquad (6)$$

2,000 to 1,000 cm^{-1}:

$$\delta_3 = 0.52971744 - 4.3521497 \times 10^{-4} \nu, \quad (7)$$

1,000 to 450 cm^{-1}:

$$\delta_3 = -0.36407533 + 8.025447 \times 10^{-4} \nu. \quad (8)$$

TABLE 2. - Data for dial calibration

Dial	Literature	Correction	Dial	Literature	Correction
4,000 to 2,000 cm^{-1} range (15)					
H_2O:			HCl:		
3,950.6	3,950.0	-0.6	3,045.2	3,045.0	-0.2
3,943.4	3,942.9	-.5	3,030.2	3,030.1	-.1
3,925.5	3,925.2	-.3	3,014.5	3,014.4	-.1
3,920.5	3,920.1	-.4	2,998.2	2,998.0	-.2
3,899.3	3,899.4	.1	2.981.1	2.981.0	-.1
3,865.4	3,865.2	-.2	2,963.5	2,963.3	-.2
3,836.0	3,835.1	-.9	2,945.2	2,944.9	-.3
3,816.9	3,816.1	-.8	2,926.2	2,925.9	-.3
3,807.9	3,807.0	-.9	2,906.5	2,906.2	-.3
3,780.3	3,779.4	-.9	2,865.4	2,865.1	-.3
3,760.5	3,759.8	-.7	2,844.0	2,843.6	-.4
3,752.5	3,752.2	-.3	2,821.9	2,821.6	-.3
3,715.2	3,714.8	-.4	2,799.1	2,798.9	-.2
3,702.8	3,701.9	-.9	2,775.9	2,775.8	-.1
3,660.5	3,659.9	-.6	2,752.2	2,752.0	-.2
3,656 .9	3,656.3	-.6	CO_2:		
3,638.7	3,638.2	-.5	2,371.1	2,371.4	.3
3,603.6	3,603.1	-.5	2,370.0	2,370.3	.3
3,577.7	3,577.1	-.6	2,367.5	2,367.9	.4
3,571.2	3,570.5	-.7	2,363.8	2,364.2	.4
3,552.9	3,552.4	-.5	2,351.3	2,351.5	.2
3,537.0	3,536.4	-.6	2,349.9	2,349.9	-
3,510.1	3,509.5	-.6	2,347.5	2,347.6	.1
3,497.0	3,496.6	-.4	2,344.2	2,344.4	.2
3,488.5	3,488.1	-.4	2,323.0	2,323.1	.1
3,482.9	3,482.3	-.6	2,321.1	2,321.2	.1
3,447.7	3,447.2	-.5	2,319.1	2,319.2	.1
			2,304.9	2,304.8	-.1
450 to 200 cm^{-1} range (17)					
H_2O:			H_2O:--		
442.13	442.0	-.13	Continued		
418.63	419.0	.37	334.60	335.1	.50
397.16	397.7	.54	327.18	327.7	.52
374.80	375.5	.70	301.55	302.8	1.25

TABLE 2. - Data for dial calibration--Continued

Dial	Literature	Correction	Dial	Literature	Correction
2,000 to 1,000 cm^{-1} range (15)			1,000 to 450 cm^{-1} range (15)		
H_2O:			NH_3:		
1,942.8	1,942.6	-0.2	971.45	971.91	0.46
1,918.35	1,918.05	-.30	951.40	951.80	.40
1,890.0	1,889.6	-.4	907.85	908.18	.33
1,869.6	1,869.4	-.2	813.95	814.24	.29
1,844.4	1,844.2	-.2	753.40	753.61	.21
1,830.4	1,830.2	-.2	CO_2:		
1,825.45	1,825.25	-.20	693.51	693.59	.08
1,810.95	1,810.6	-.35	683.85	683.96	.11
1,799.95	1,799.60	-.35	675.89	676.04	.15
1,792.9	1,792.6	-.3	672.76	672.88	.12
1,791,35	1,790.95	-.40	671.05	671.34	.29
NH_3:			662.52	662.71	.19
1,177.05	1,177.09	.04	660.97	661.17	.20
1,158.90	1,158.95	.05	659.31	659.60	.29
1,140.60	1,140.64	.04	657.85	658.07	.22
1,122.15	1,122.14	-.01	656.32	656.53	.21
1,103.45	1,103.44	-.01	648.71	648.90	.19
1,084.50	1,084.61	.11	647.20	647.39	.19
1,065.45	1,065.57	.12	639.71	639 .83	.12
1,046.35	1,046.41	.06	638.12	638.34	.22

These corrections were incorporated into the computer program. Although the shrinkage and grid corrections are based on misalinement-corrected (that is, 90 percent T baseline) data, the absolute calibration of the dial embodied in equations (6 to 8) is independent of any chart corrections.

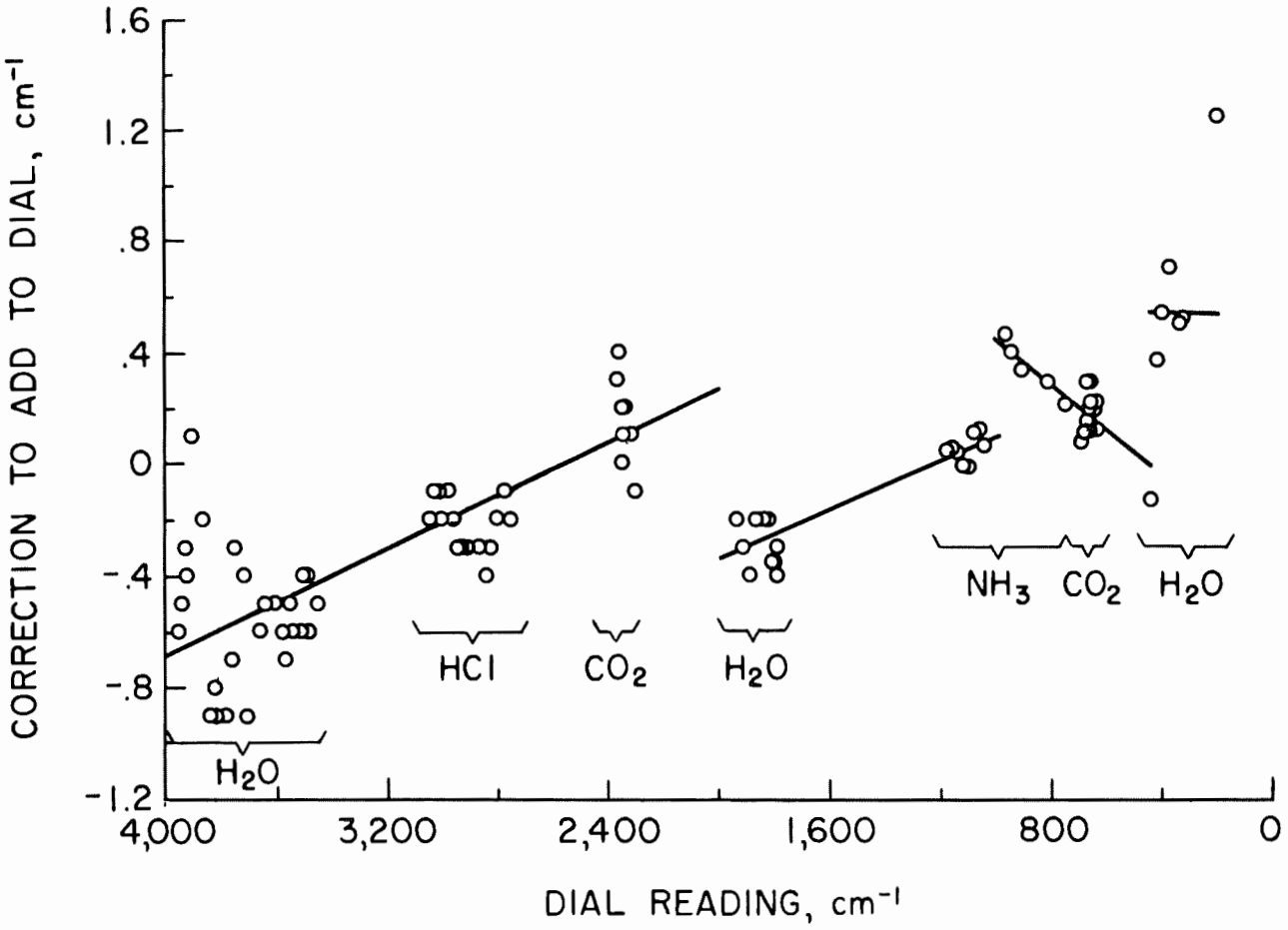

FIGURE 3. - Corrections for wave number dial.

Table 3 gives typical results obtained from the correction program at this stage of its development and indicates the general magnitude and behavior of the corrections applied.

In order to obtain a reliable estimate of the precision to be expected in recorded spectra, three spectra of the same polystyrene film specimen were run, each being independent of the others in regard to setting up the instrument, mounting the chart paper, and positioning the pen at the start of the trace. The agreement between these should be a proper measure of the reproducibility achieved with respect to all those variables which are subject to operator judgment in running and reading a spectrum, as well as the practical repeatability of the instrument. Band positions were estimated from the charts to the nearest 1 wave number, after removing the chart from the instrument. Sometimes a desk-top magnifier with built-in micrometer scale was used, especially at a higher wave number where the chart readability is poorer. The results from each run are given in table 4.

TABLE 3. - Polystyrene spectrum corrected as described in text

(all values in cm^{-1})

Chart reading	Corrections					Corrected value
	Misalinement	Shrinkage	Grid	Dial	Total	
3,096.0	3.95	-0.09	0.10	-0.26	3.70	3,099.7
3,077.0	4.50	-.05	.10	-.25	4.30	3,081.3
3,054.0	4.63	-.00	.11	-.24	4.50	3,058.5
3,018.0	4.70	.08	.11	-.22	4.67	3,022.7
2,999.0	4.11	.12	.12	-.22	4.13	3,003.1
2,911.0	4.55	.31	.13	-.17	4.82	2,915.8
2,841.0	4.16	.47	.14	-.14	4.63	2,845.6
1,939.0	1.04	.23	.13	-.32	1.08	1,940.1
1,868.0	.90	.33	.04	-.29	.98	1,869.0
1,799.0	.89	.42	-.04	-.25	1.02	1,800.0
1,598.0	1.04	.69	-.18	-.17	1.38	1,599.4
1,581.0	.97	.71	-.18	-.16	1.34	1,582.3
1,490.0	1.02	.83	-.20	-.12	1.53	1,491.5
1,448.0	1.00	.89	-.20	-.11	1.58	1,449.6
1,179.0	.80	1.25	-.06	.02	2.01	1,181.0
1,152.0	.79	1.28	-.03	.02	2.06	1,154.1
1,066.0	.74	1.40	.07	.07	2.28	1,068.3
1.025.0	.70	1.45	.13	.08	2.36	1,027.4
904.0	.66	1.30	.02	.37	2.35	906.3
839.0	.67	1.33	-.04	.31	2.27	841.3
753.0	.61	1.38	-.09	.24	2.14	755.1
697.0	.57	1.42	-.10	.20	2.09	699.1

TABLE 4. - Polystyrene chart data[1]

Band	Run 1		Run 2		Run 3	
	ν, cm^{-1}	T, percent	ν, cm^{-1}	T, percent	ν, cm^{-1}	T, percent
1.....	3,096	37	3,096	38	3,097	38
2.....	3,077	9	3,077	9	3,077	10
3.....	3,052	4	3,054	4	3,053	4
4.....	3,018	1	3,018	1	3,018	1
5.....	2,998	22	2,999	23	2,999	23
[2]6.....	2,912	0	2,911	1	2,913	1
7.....	2,842	10	2,841	10	2,842	10
8.....	1,939	52	1,939	52	1,941	51
[2]9.....	1,867	63	1,868	62	1,868	62
10.....	1,799	61	1,799	61	1,799	60
11.....	1,598	5	1,598	5	1,599	5
12.....	1,581	31	1,581	32	1,581	31
13.....	1,490	1	1,490	1	1,491	1
14.....	1,448	1	1,448	1	1,449	1
15.....	1,179	42	1,179	43	1,179	42
16.....	1,152	41	1,152	41	1,152	40
17.....	1,066	33	1,066	33	1,067	33
18.....	1,026	13	1,025	13	1,026	13

See footnotes at end of table.

TABLE 4. - Polystyrene chart data[1]--Continued

Band	Run 1		Run 2		Run 3	
	ν, cm^{-1}	T, percent	ν, cm^{-1}	T, percent	ν, cm^{-1}	T, percent
19.....	904	28	904	28	905	28
20.....	839	55	839	54	840	53
[2]21.....	754	1	753	1	754	1
[2]22.....	697	1	697	1	698	1

[1] Readings directly from charts.
[2] Peak not sharply defined.

In order to evaluate the possible effect of personal bias in reading the charts, they were read independently by another observer. Table 5 summarizes the intercomparisons made. The chart scale is such that the readability is no better than ±0.5 wave number over the 2,000 to 200-cm^{-1} range and ±1 wave number over the 4,000 to 2,000-cm^{-1} range (that is, to the nearest one-tenth of the distance between adjacent reticle lines in both cases), with reasonable care.

TABLE 5.-- Analysis of variability in polystyrene band positions read from charts

	2 different observers reading same 3 charts			3 different charts read by same observer	
	Chart 1	Chart 2	Chart 3	Observer 1	Observer 2
Percent of identical values.....	64	71	64	50	45
Percent of values differing by 1 cm^{-1}....	29	29	29	43	48
Percent of values differing by 2 cm^{-1}....	7	0	7	7	7

On the basis of this data, the following is concluded:

1. There is no significant personal bias in the data given in table 4, since the differences between independent observers reading the same chart are smaller than the differences between triplicate charts read by the same observer.

2. The differences in chart values between triplicate charts are somewhat greater than can be accounted for on the basis of chart readability.

3. Absorption band intensities (that is, percent transmittance values) are satisfactorily reproducible.

The nature of the correction program developed is such that only the shrinkage correction could lead to a change in the apparent precision of triplicate runs after correction. Table 6 lists corrected values for the data in table 4. Comparing the three runs with one another, the following relationships are found:

Percent of values differing by 0 to 0.5 cm^{-1} = 64

Percent of values differing by 0.6 to 1.5 cm^{-1} = 30

Percent of values differing by 1.6 to 2.0 cm^{-1} = 6

From the data in table 5 it is clear that the shrinkage correction (which is formulated independently for each chart) has removed most of the variability between the triplicate runs and, in fact, reduced it to the level characteristic of the inherent chart readability. This is as it should be.

TABLE 6. - Polystyrene bands, corrected as described in text

Band[1]	Corrected values, cm^{-1}		
	Run 1	Run 2	Run 3
1	3,100.0	3,099.7	3,100.7
2	3,081.6	3,081.3	3,081.3
3	3,056.8	3,058.5	3,057.5
4	3,022.9	3,022.7	3,022.7
5	3,002.4	3,003.1	3,003.1
6	2,917.1	2,915.8	2,917.8
7	2,846.9	2,845.6	2,846.6
8	1,940.2	1,940.1	1,941.8
9	1,868.0	1,869.0	1,868.6
10	1,800.1	1,800.0	1,799.6
11	1,599.5	1,599.4	1,599.8
12	1,582.4	1,582.3	1,581.7
13	1,491.6	1,491.5	1,491.8
14	1,449.7	1,449.6	1,499.8
15	1,181.1	1,181.0	1,179.9
16	1,154.2	1,154.1	1,153.0
17	1,068.4	1,068.3	1,068.1
18	1,028.4	1,027.4	1,027.1
19	906.6	906.3	906.3
20	841.6	841.3	841.3
21	756.6	755.1	755.3
22	699.6	699.1	699.4

[1] Band designations as in table 4.

Polystyrene calibration bands that have been reported in the literature are summarized in table 7. All of the bands listed for polystyrene in reference 15 are shown here, except bands 6 and 8. The wave numbers for these two bands were listed with a higher uncertainty (±2 and ±1, respectively) and the more recent values in reference 11 were considered better. The other bands given in table 7 are not listed in reference 15 and were taken from reference 14 or 11 giving preference to reference 11 in cases where a choice had to be made. There are significant discrepancies among the values quoted in the literature for several band positions. The most serious discrepancies encountered are listed in table 8. A critical review of the literature data was not attempted.

TABLE 7. - Polystyrene calibration bands cited in literature

(All values, in vacuo, quoted (wavelength or wave number) from reference indicated)

Band[1]	Wavelength, μm	Wave number, cm^{-1}	References
1.....	-	3,104.4	14
2.....	-	3,082.6	14
3.....	-	3,060.5	14
4.....	-	3,027.1 ±0.3	15
5.....	-	3,002.8	14
6.....	3.423	-	11
7.....	-	2,850.7 ±0.3	15
8.....	5.145	-	11
9.....	-	1,871.0 ±0.3	15
10.....	-	1,801.6 ±0.3	15
11.....	-	1,601.4 ±0.3	15
12.....	-	1,583.1 ±0.3	15
13.....	6.697	-	11
14.....	6.893	-	11
15.....	-	1,181.4 ±0.3	15
16.....	-	1,154.3 ±0.3	15
17.....	-	1,069.1 ±0.3	15
18.....	-	1,028.0 ±0.3	15
19.....	-	906.7 ±0.3	15
20.....	11.886	-	11
21.....	13.240	-	11
22.....	-	698.9 ±0.5	15

[1] Band designations as in table 4.

TABLE 8. - Discrepancies in band positions quoted by different authors

(Values are wave numbers, in vacuo)

Band[1]	References		
	14	[2]11	15
4.....	3,026.5	-	3,027.1 ±0.3
6.....	2,924.2	2,921.4	2,924 ±2
8.....	1,945.8	1,943.6	1,944.0 ±1
11.....	1,602.7	1,601.3	1,601.4 ±0.3
13.....	1,494.9	1,493.2	-
16.....	-	1,153.7	1,154.3 ±0.3

[1] Band designations as in table 4.

[2] Original text quotes wavelengths, in vacuo.

The best estimate of band positions for polystyrene from our data are the averages of the three corrected values given previously. These are listed in the second column of table 9. The last column gives the differences between our values and those quoted in the literature and indicates that our values are almost uniformly too low, by an amount which exceeds the expected experimental error in several instances.

TABLE 9. - Comparison of values for polystyrene band positions

(All values in cm^{-1})

Band[1]	This work[2]	Literature value	Difference
1.....	3,100.1	3,104.4 (14)	-4.3
2.....	3,081.4	3,082.6 (14)	-1.2
3.....	3,057.6	3,060.5 (14)	-2.9
4.....	3,022.8	3,027.1 (15)	-4.3
5.....	3,002.9	3,002.8 (14)	.1
6.....	2,916.9	2,921.4 (11)	-4.5
7.....	2,846.4	2,850.7 (15)	-4.3
8.....	1,940.7	1,943.6 (11)	-2.9
9.....	1,868.6	1,871.0 (15)	-2.4
10.....	1,799.9	1,801.6 (15)	-1.7
11.....	1,599.5	1,601.4 (15)	-1.9
12.....	1,582.1	1,583.1 (15)	-1.0
13.....	1,491.6	1,493.2 (11)	-1.6
14.....	1,449.7	1,450.7 (11)	-1.0
15.....	1,180.7	1,181.4 (15)	-.7
16.....	1,153.7	1,154.3 (15)	-.6
17.....	1,068.3	1,069.1 (15)	-.8
18.....	1,027.6	1,028.0 (15)	-.4
19.....	906.4	906.7 (15)	-.3
20.....	841.4	841.3 (11)	.1
21.....	755.7	755.3 (11)	.4
22.....	699.4	698.9 (15)	.5

[1]Band designations as in table 4.
[2]Average of 3 values in table 6.

It is well known that, for a spectrum obtained using a continuous scan, apparent band positions can be in error in the direction of the scan because of the noninstantaneous response of the recording system. A suppression circuit, such as used in the subject instrument, tends to minimize this error by automatically decreasing the scan rate when large changes in transmission are encountered, but there is no guarantee that the instrument settings used permitted full compensation. All of the spectra reported herein, including those for the polystyrene specimen, were run at the same instrument settings the particular values used being the best compromise between slow scanning rates (for good band definition) and a reasonable length of time to obtain a completed spectrum. With the settings used, between 3 and 4 hours were required to run a spectrum, depending on the number of bands appearing in it. Although it was thought that these settings were adequate to reduce scanning rate errors to a negligible level, this may not have been the case. The differences in the last column of table 9 are consistent with an error of this kind. The instrument scans in the direction of decreasing wave number and, for given instrument settings, scans larger wave numbers faster than smaller. For the settings used, average scanning rates for the various ranges, with the suppression circuit disabled, were as follows:

Range, cm^{-1}	Approximate average rate, cm^{-1}/min
4,000 - 2,000	77
2,000 - 1,000	36
1,000 - 450	13
450 - 200	7

Since many of the polystyrene bands are relatively broad and there are discrepancies in the literature regarding band positions for this material, it was considered advisable to obtain spectra for another material which has established band positions. Indene was chosen for this purpose. Being a liquid at room temperature, it is somewhat less convenient to work with, but its spectrum has numerous bands over the range of interest here. A film of the liquid between two KBr disks was used as the specimen with teflon spacers to obtain varying film thicknesses. The spectra were run using the same instrument settings as for all other materials and the data was processed using the same correction program. The results are summarized in table 10. As for the polystyrene data, our corrected band positions tend to be low and by an amount which generally decreases with decreasing wave number (that is, decreasing scan rate). As a final test, three polystyrene and three indene bands were determined manually by recording dial readings which produced the same percent transmittance on each side of the band minima and taking the average of these to be the correct band position. In these cases, there can be no question of scanning-rate errors affecting the determinations. The results are given in table 11.

TABLE 10. - Indene absorption bands

(All values in cm^{-1}, in vacuo)

Band[1]	Corrected	Literature[1]	-(Difference)	Band[1]	Corrected	Literature[1]	-(Difference)
1	3,922.9	3,926.5	3.6	42	1,855.0	1,856.7	1.7
2	3,898.2	3,900.7	2.5	43	1,823.7	1,825.5	1.8
3	3,796.1	3,797.5	1.4	44	1,793.7	1,796.9	3.2
4	3,741.9	3,747.5	4.6	48	1,608.4	1,609.6	1.2
5	3,656.7	3,656.7	.0	49	1,586.77	1,587.7	1.93
8	3,292.9	3,297.0	4.1	51	1,551.14	1,553.3	2.16
9	3,135.3	3,139.5	4.2	53	1,456.52	1,457.8	1.28
10	3,106.6	3,110.0	3.4	54	1,392.20	1,393.2	1.00
11	3,063.9	3,068.5	4.6	55	1,359.87	1,361.3	1.43
12	3,022.0	3,025.6	3.6	56	1,329.59	1,332.5	2.91
15	2,885.0	2,887.0	2.0	57	1,311.50	1,312.5	1.00
17	2,767.3	2,771.0	3.7	58	1,287.06	1,287.8	.74
19	2,670.1	2,673.7	3.6	59	1,262.54	1,263.8	1.26
21	2,594.5	2,598.6	4.1	60	1,225.18	1,226.2	1.02
22	2,554.8	2,558.5	3.6	61	1,204.47	1,205.2	.73
23	2,522.8	2,525.9	3.1	62	1,165.23	1,166.2	.97
25	2,464.3	2,465.6	1.3	64	1,121.30	1,122.7	1.40
26	2,435.7	2,439.5	3.8	65	1,104.42	1,106.4	1.98
28	2,300.7	2,304.8	4.1	66	1,066.79	1,067.9	1.11
33	2,169.1	2,172.8	3.7	67	1,017.55	1,018.6	1.05
34	2,133.6	2,135.8	2.2	71	913.84	914.8	.96
35	2,109.8	2,113.5	3.7	72	860.88	861.3	.42
36	2,086.0	2,090.2	4.2	73	829.74	830.5	.76
37	2,044.6	2,049.6	5.0	74	764.60	765.4	.80
39	1,940.1	1,943.2	3.1	75	729.40	730.1	.70
40	1,911.8	1,915.0	3.2	76	717.15	718.2	1.05
41	1,882.8	1,884.5	1.7	77	691.49	692.8	1.31

[1]As given in reference 15.

TABLE 11. - Band positions determined manually

(All values in cm^{-1}, in vacuo)

Material	Dial reading	Dial correction	Corrected value	Literature
Indene.....	3,067.2 - 3,068.9	-0.2	3,067.8 ±0.8	3,068.5 ±2.5
Indene.....	3,025.0 - 3,025.2	-.2	3,024.9 ±0.1	3,025.6 ±0.5
Polystyrene.....	2,847.4 - 2,852.8	-.1	2,850.0 ±1.7	2,850.7 ±0.3
Polystyrene.....	1,599.4 - 1,603.0	-.2	1,601.0 ±1.8	1,601.4 ±0.3
Indene.....	1,457.2 - 1,457.5	-.1	1,457.2 ±0.2	1,457.8 ±0.5
Polystyrene.....	839.0 - 843.7	+.3	841.6 ±2.4	841.32

These results confirm the existence of a scanning-rate error in the chart data.

A composite summary of the scanning-rate errors is shown graphically in figure 4. The curve shown has the equation

$$\delta_{\nu} = -2.44258 + 3.9149426 \times 10^{-2}\ \nu - 6.6642447 \times 10^{-7}\ \nu^2, \qquad (9)$$

and is our best estimate of the magnitude of the correction which must be added to account for scanning-rate errors in the chart data. Most of the values fall within an uncertainty band of ±1 cm^{-1}. The scatter of the points, especially in the high wave number region, is greater than one would like, but efforts to improve the quantitative correlation of the correction by including parameters characteristic of the band shapes or heights were mainly unsuccessful. A careful analysis of the charts did reveal that those points which

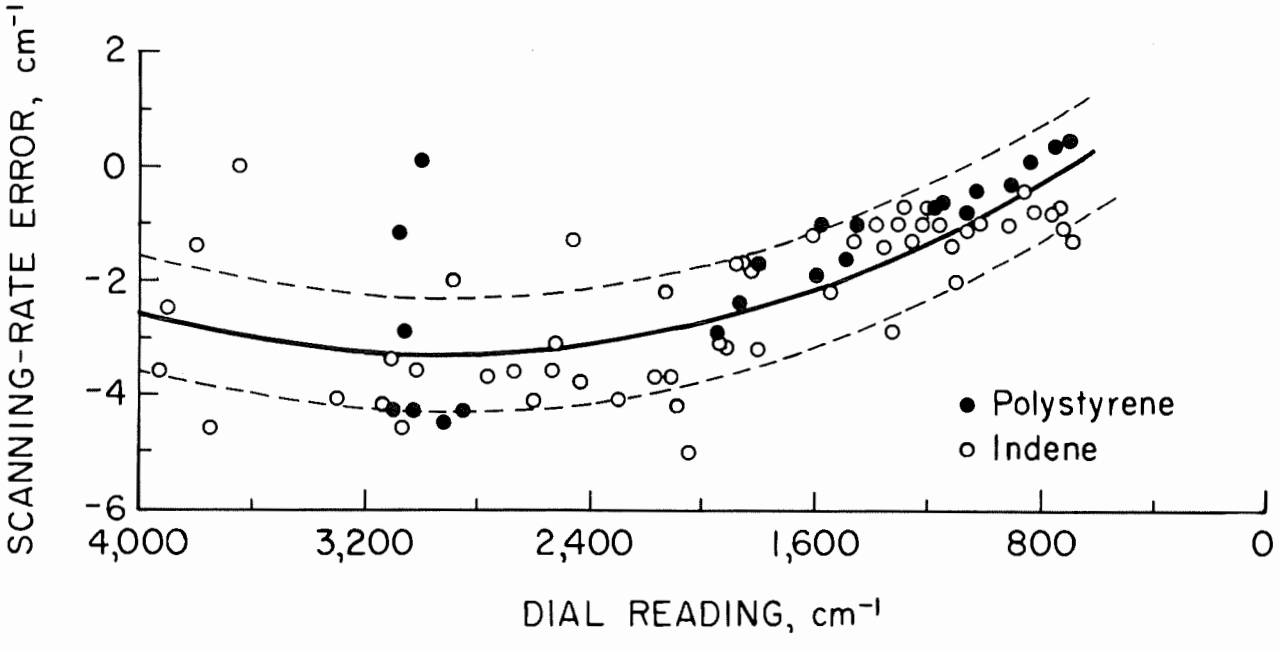

FIGURE 4. - Composite summary of scanning-rate errors in chart data.

deviate the most from the fitted curve were obtained from bands which are weak (change in transmittance of 15 percent or less) or broad at the band minimum.

Equation (9) was incorporated into the computer program and chart data from all of the spectra reported herein was processed using it. The resulting wave numbers for selected bands are shown on the charts. The selection rules used, though qualitative, represent an effort to report only those band positions which we feel are reliable within certain limits. For large, sharp bands, we believe the numerical values shown are accurate to within ± 1 cm^{-1} on an absolute basis. For weaker (less than 20 percent change in transmittance relative to the baseline in the immediate vicinity of the band) or broader bands, error limits of ± 2 cm^{-1} are more realistic. Bands considered unimportant or less certain than ± 2 cm^{-1} for whatever reason have not been assigned numerical values.

REFERENCE SPECTRA

An index to the reference spectra is given in table 12. It should be noted that the total correction made in correcting the chart reading of a given absorption band position to its near absolute value was at times as great as 9 to 10 wave numbers. Hence, the band labels may differ from corresponding chart readings up to this amount.

TABLE 12. - Index to infrared spectra

Compound	Formula or source	Spectrum
Lead ethyl xanthate	$(C_2H_5OCS_2)_2Pb$	1
Lead n-propyl xanthate	$(C_3H_7OCS_2)_2Pb$	2
Lead isopropyl xanthate	$[(CH_3)_2CHOCS_2]_2Pb$	3
Lead n-butyl xanthate	$(C_4H_9OCS_2)_2Pb$	4
Lead isobutyl xanthate	$[(CH_3)_2CHCH_2OCS_2]_2Pb$	5
Lead n-amyl xanthate	$(C_5H_{11}OCS_2)_2Pb$	6
Zinc ethyl xanthate	$(C_2H_5OCS_2)_2Zn$	7
Zinc n-propyl xanthate	$(C_3H_7OCS_2)_2Zn$	8
Zinc isopropyl xanthate	$[(CH_3)_2CHOCS_2]_2Zn$	9
Zinc n-butyl xanthate	$(C_4H_9OCS_2)_2Zn$	10
Zinc isobutyl xanthate	$[(CH_3)_2CHCH_2OCS_2]_2Zn$	11
Zinc secondary-butyl xanthate	$[(C_2H_5)CH_3CHOCS_2]_2Zn$	12
Zinc n-amyl xanthate	$(C_5H_{11}OCS_2)_2Zn$	13
Potassium ethyl xanthate	$C_2H_5OCS_2K$	14
Potassium n-propyl xanthate	$C_3H_7OCS_2K$	15
Potassium isopropyl xanthate	$(CH_3)_2CHOCS_2K$	16
Potassium n-butyl xanthate	$C_4H_9OCS_2K$	17
Potassium isobutyl xanthate	$(CH_3)_2CHCH_2OCS_2K$	18
Potassium secondary-butyl xanthate	$(C_2H_5)CH_3CHOCS_2K$	19
Potassium n-amyl xanthate	$C_5H_{11}OCS_2K$	20
Di-ethyl dixanthogen	$(C_2H_5OCS_2)_2$	21
Di-n-propyl dixanthogen	$(C_3H_7OCS_2)_2$	22

TABLE 12. - Index to infrared spectra--Continued

Compound	Formula or source	Spectrum
Di-isopropyl dixanthogen	$[(CH_3)_2CHOCS_2]_2$	23
Di-n-butyl dixanthogen	$(C_4H_9OCS_2)_2$	24
Di-isobutyl dixanthogen	$[(CH_3)_2CHCH_2OCS_2]_2$	25
Di-secondary-butyl dixanthogen	$[(C_2H_5)CH_3CHOCS_2]_2$	26
Di-n-amyl dixanthogen	$(C_5H_{11}OCS_2)_2$	27
Lead sulfate	$PbSO_4$	28
Lead thiosulfate	PbS_2O_3	29
Lead sulfite	$PbSO_3$	30
Lead carbonate	$PbCO_3$	31
Lead carbonate, basic	$(PbCO_3)_2Pb(OH)_2$	32
Sodium thiosulfate	$Na_2S_2O_3$	33
Sodium sulfite	Na_2SO_3	34
Cuprous ethyl xanthate	$C_2H_5OCS_2Cu$	35
Sodium isopropyl xanthate	$(CH_3)_2CHOCS_2Na$ (Dow Z-11)	36
Sodium isobutyl xanthate	$(CH_3)_2CHCH_2OCS_2Na$ (AERO 317)	37
Potassium amyl xanthate	$C_5H_{11}OCS_2K$ (AERO 350)	38
Potassium hexyl xanthate	$C_6H_{13}OCS_2K$ (Dow Z-10)	39

The spectra follow (figs. 5-24).

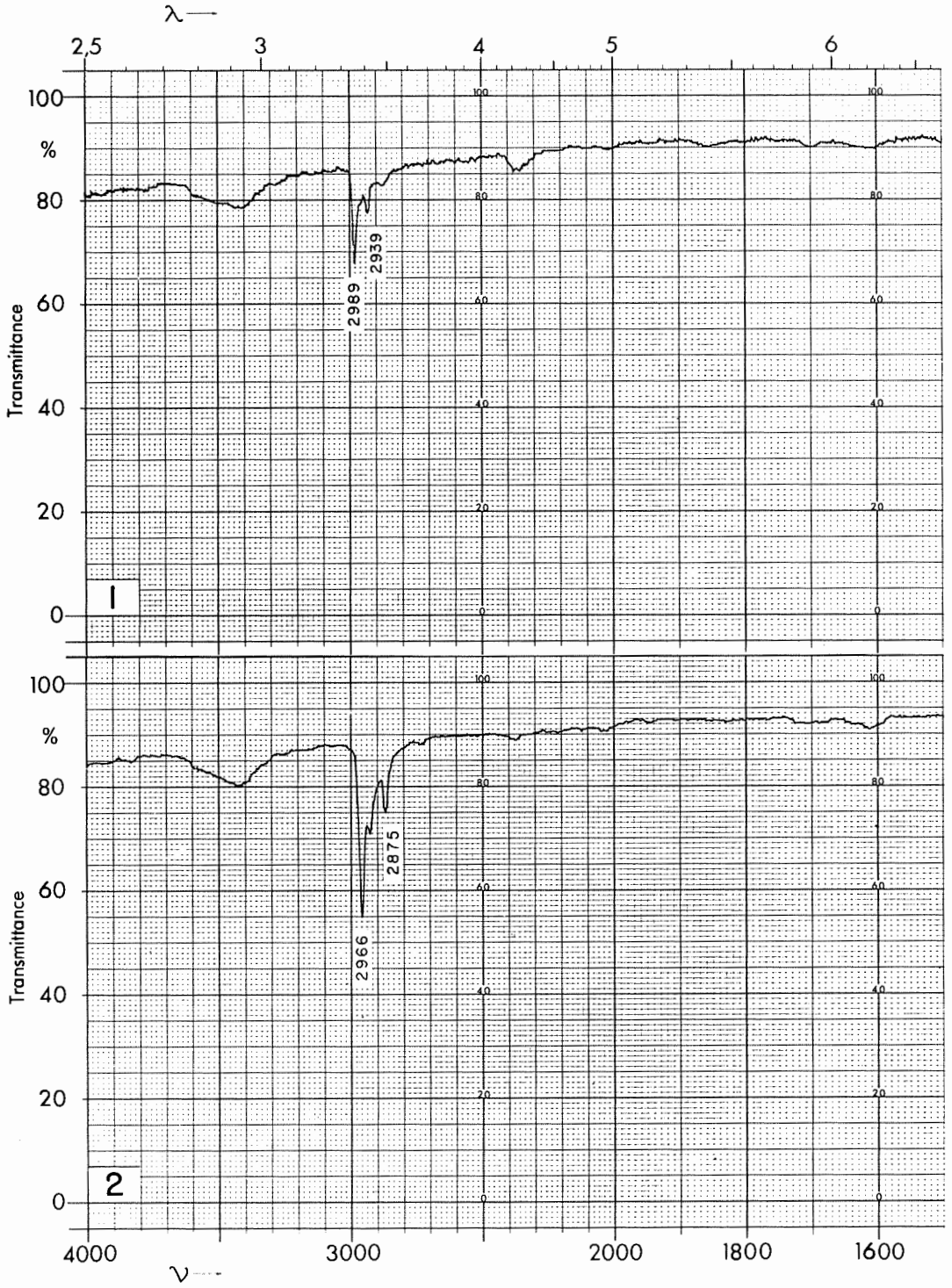

FIGURE 5. - Spectra of (1) lead ethyl xanthate and (2) lead n-propyl xanthate.

FIGURE 5. - Spectra of (1) lead ethyl xanthate and (2) lead n-propyl xanthate.–Continued

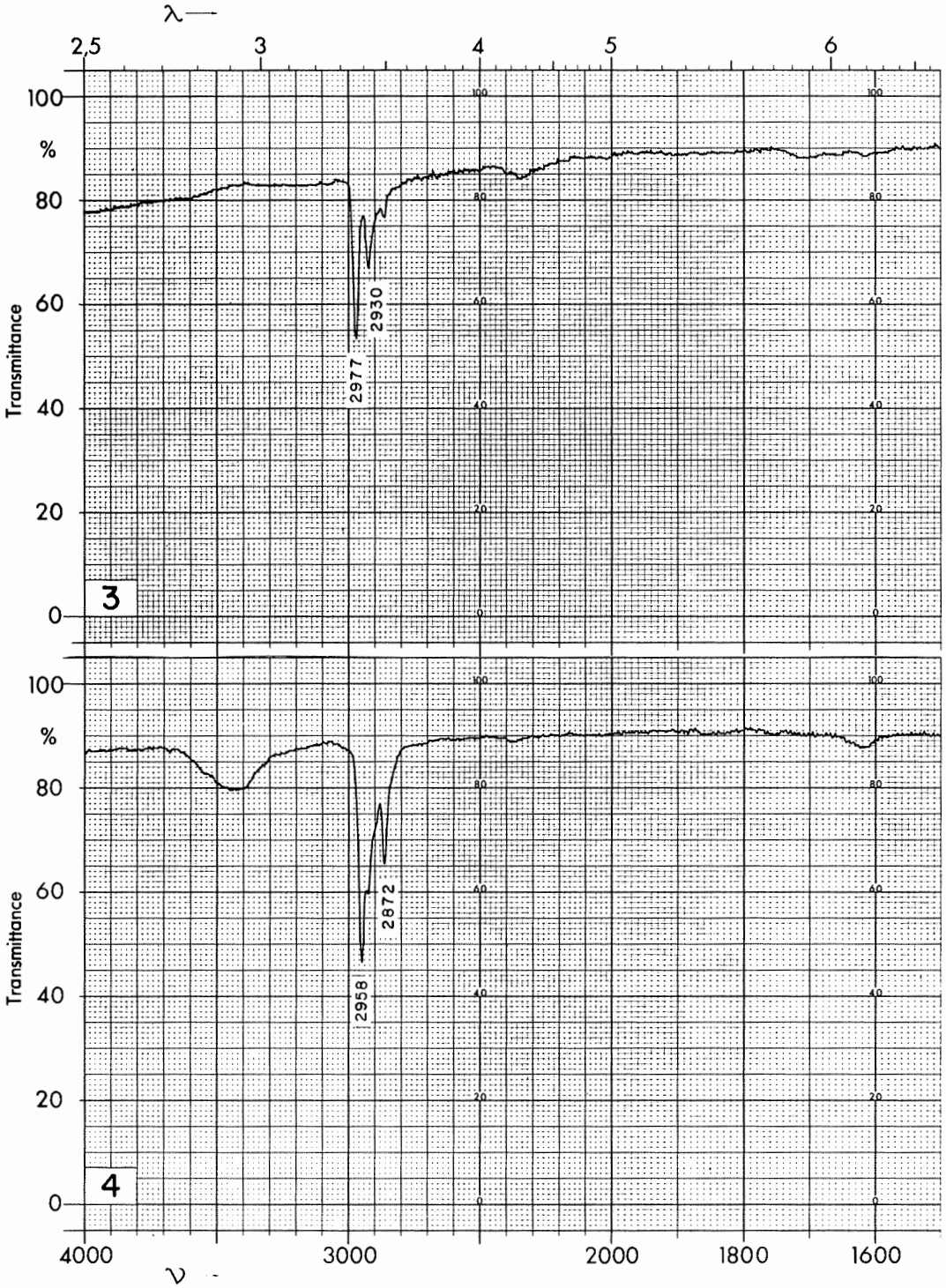

FIGURE 6. - Spectra of (3) lead isopropyl xanthate and (4) lead n-butyl xanthate.

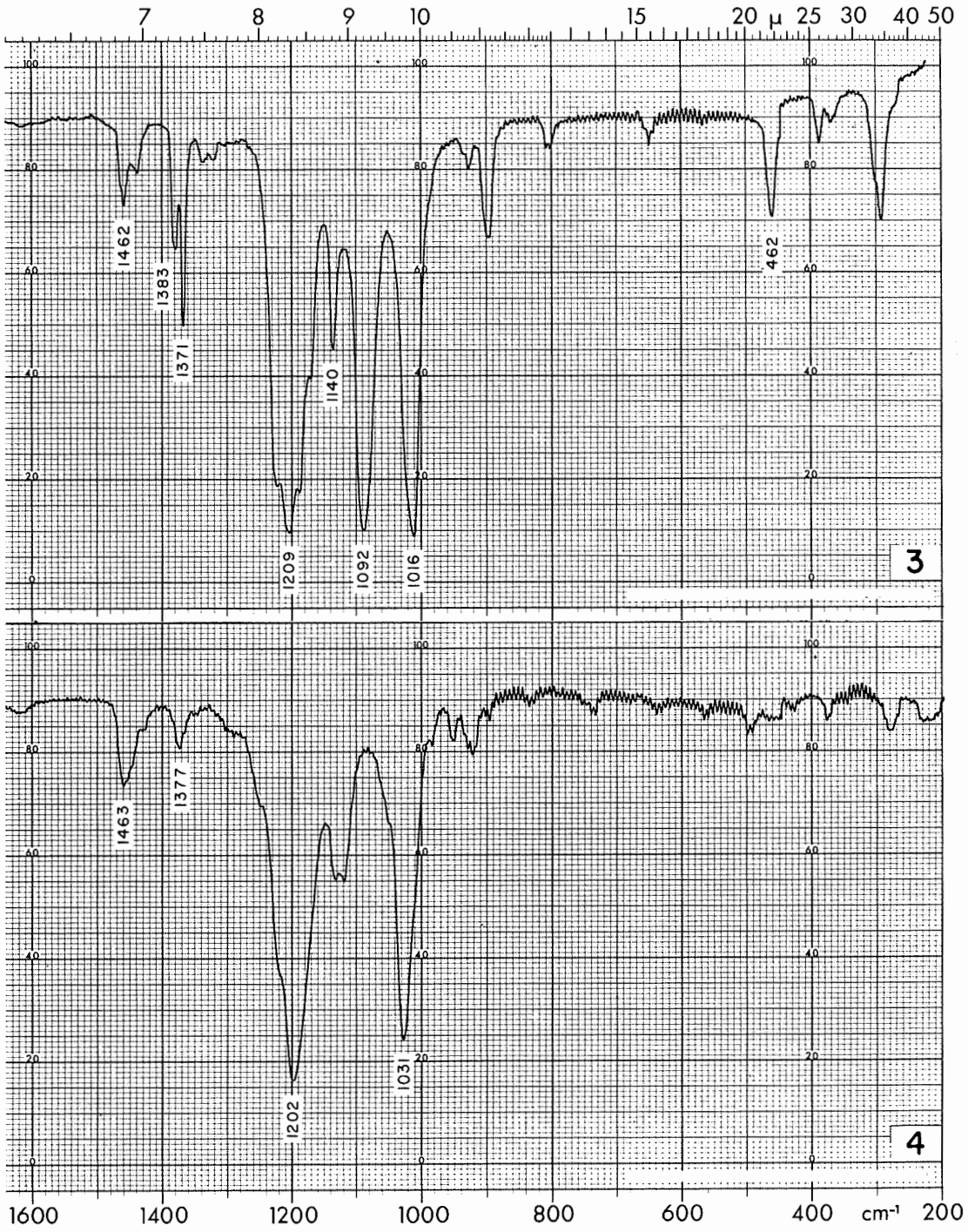

FIGURE 6. - Spectra of (3) lead isopropyl xanthate and (4) lead n-butyl xanthate.–Continued

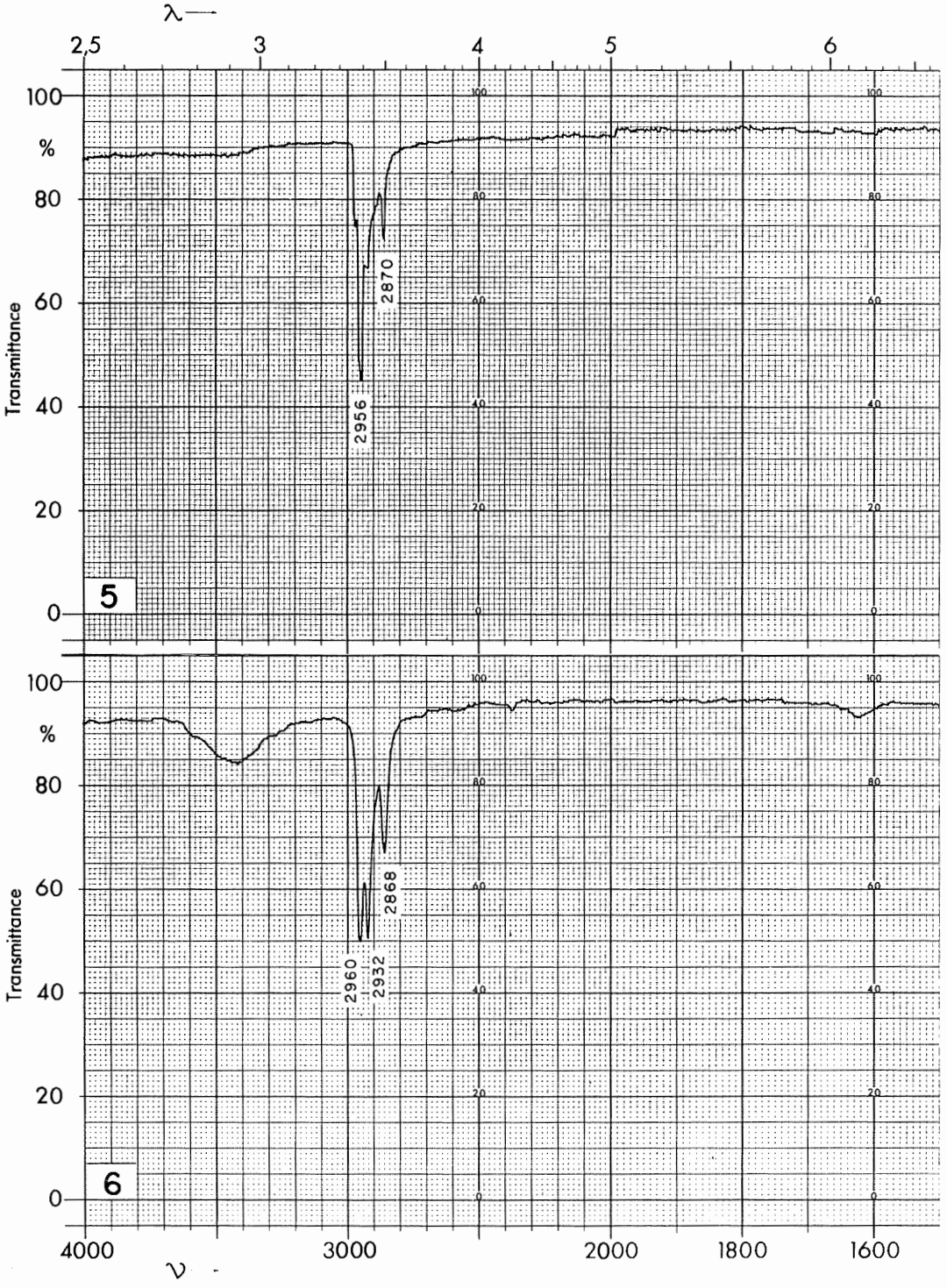

FIGURE 7. - Spectra of (5) lead isobutyl xanthate and (6) lead n-amyl xanthate.

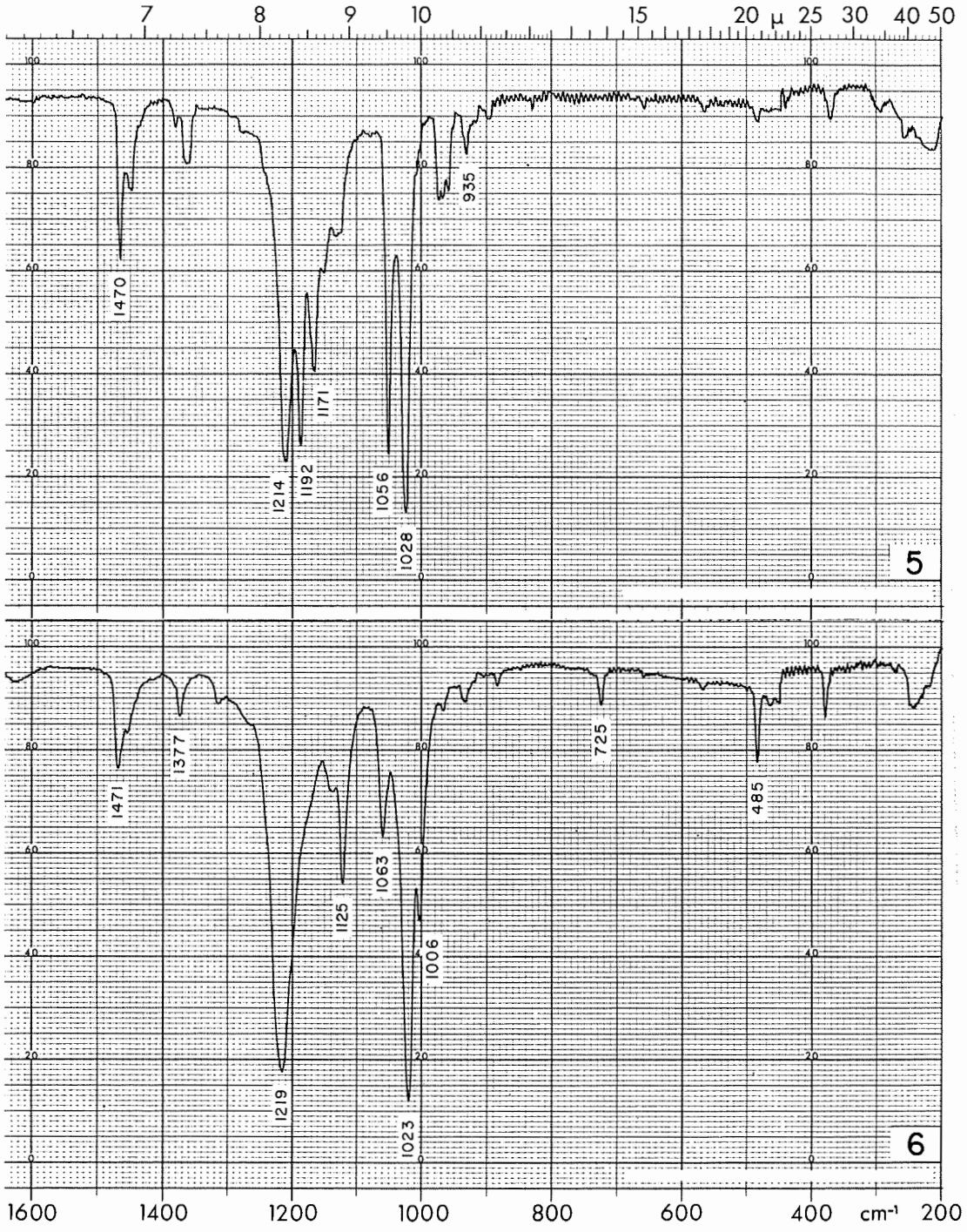

FIGURE 7. - Spectra of (5) lead isobutyl xanthate and (6) lead n-amyl xanthate.–Continued

FIGURE 8. - Spectra of (7) zinc ethyl xanthate and (8) zinc n-propyl xanthate.

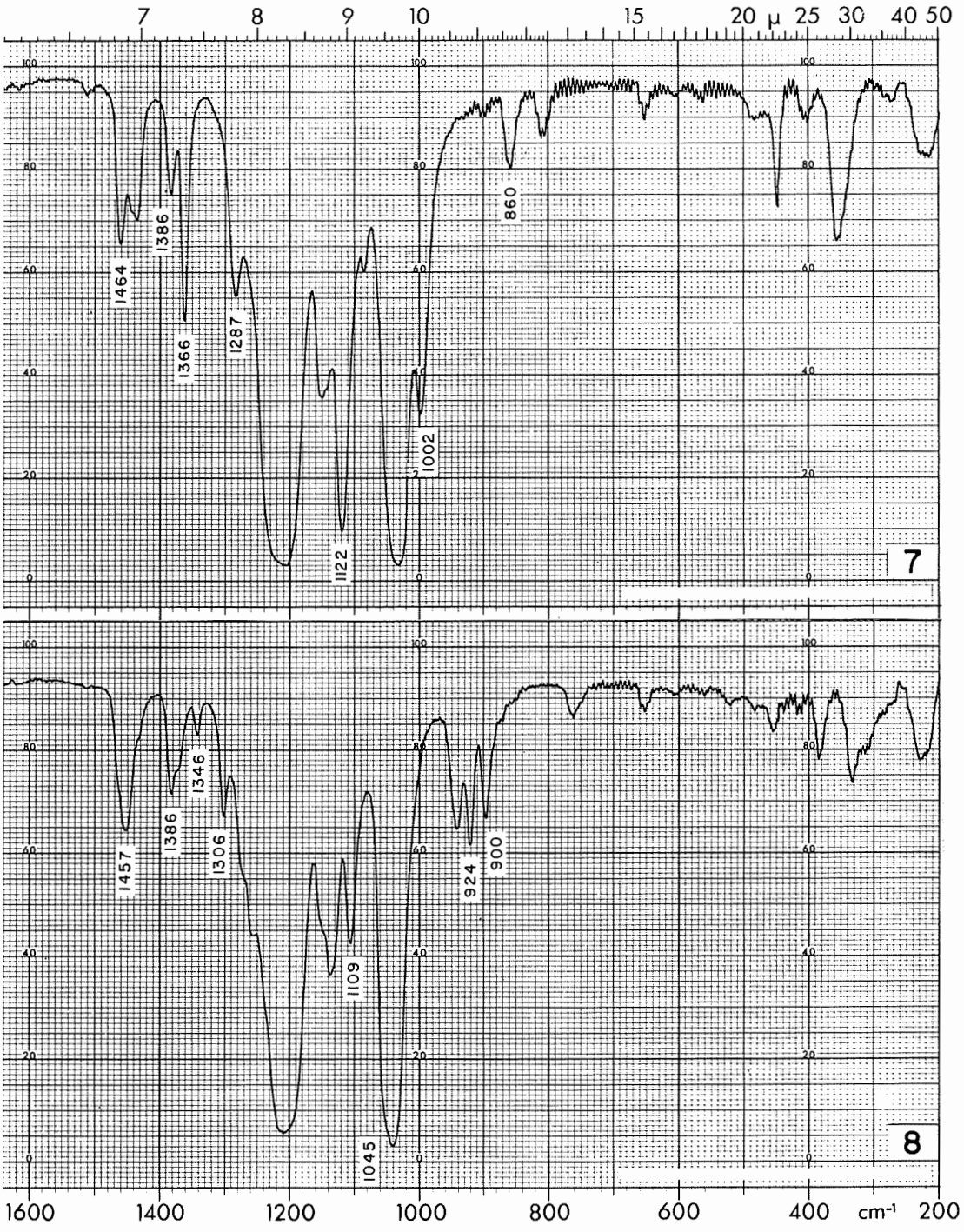

FIGURE 8. - Spectra of (7) zinc ethyl xanthate and (8) zinc n-propyl xanthate.–Continued

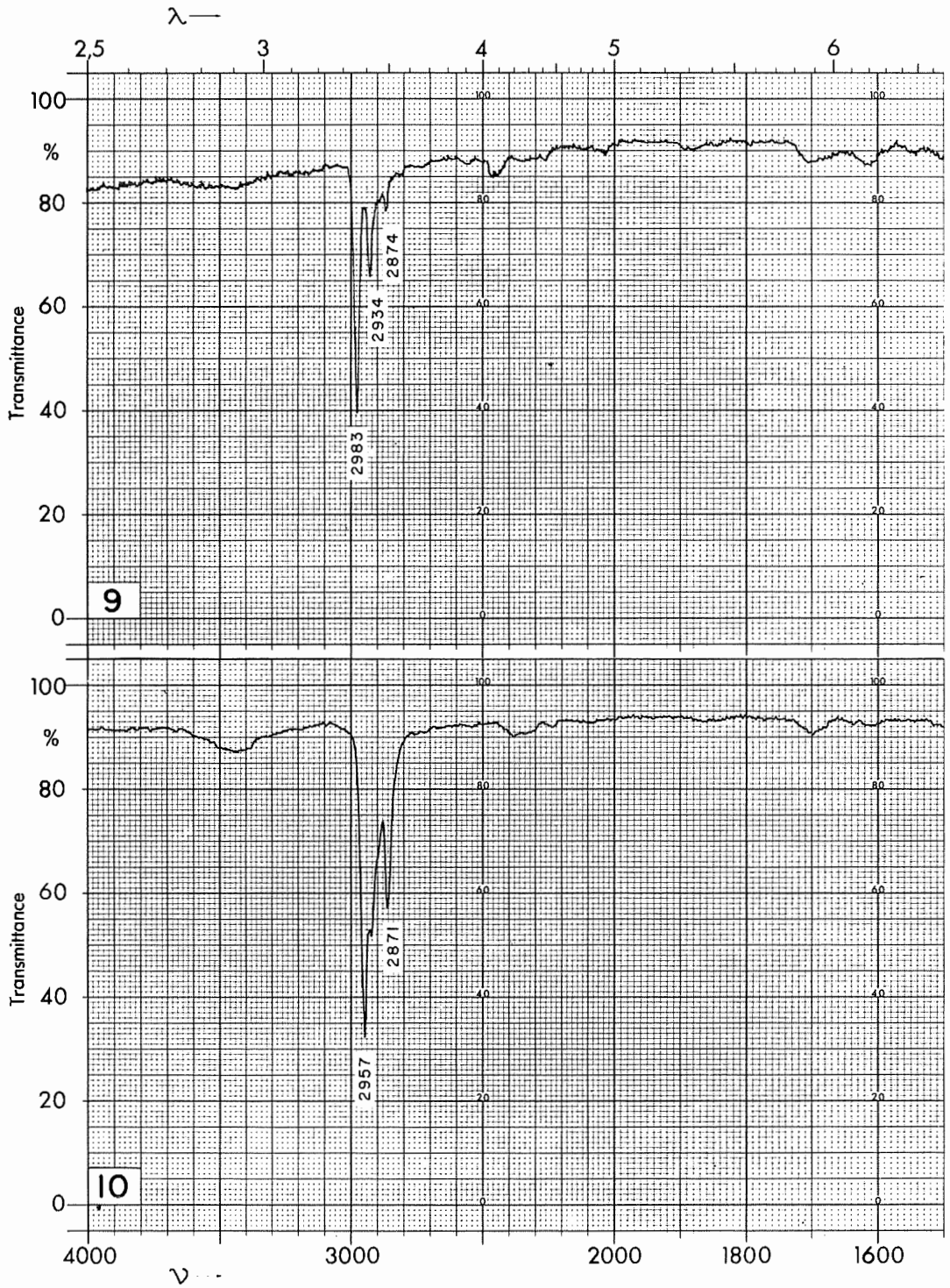

FIGURE 9. - Spectra of (9) zinc isopropyl xanthate and (10) zinc n-butyl xanthate.

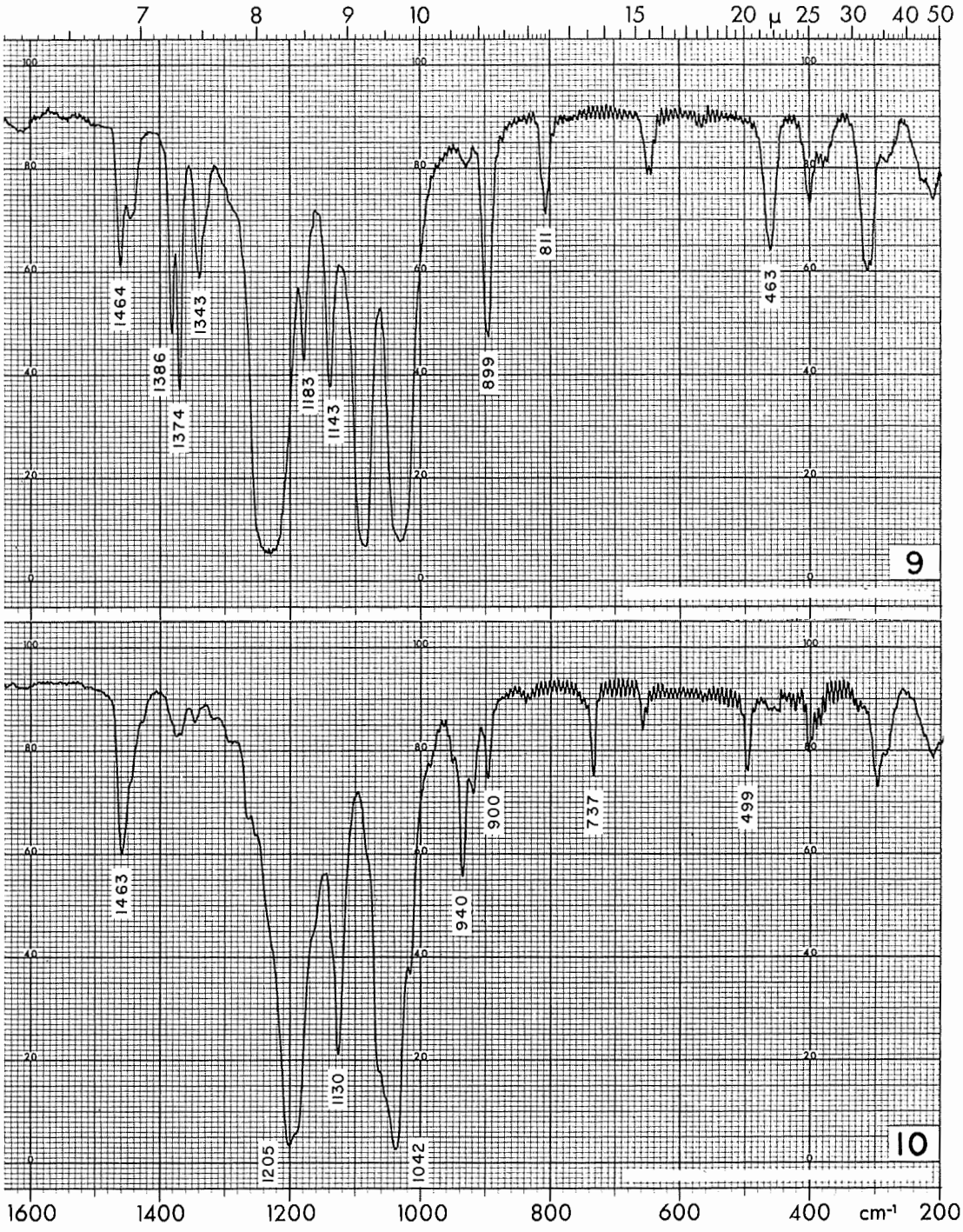

FIGURE 9. - Spectra of (9) zinc isopropyl xanthate and (10) zinc n-butyl xanthate.–Continued

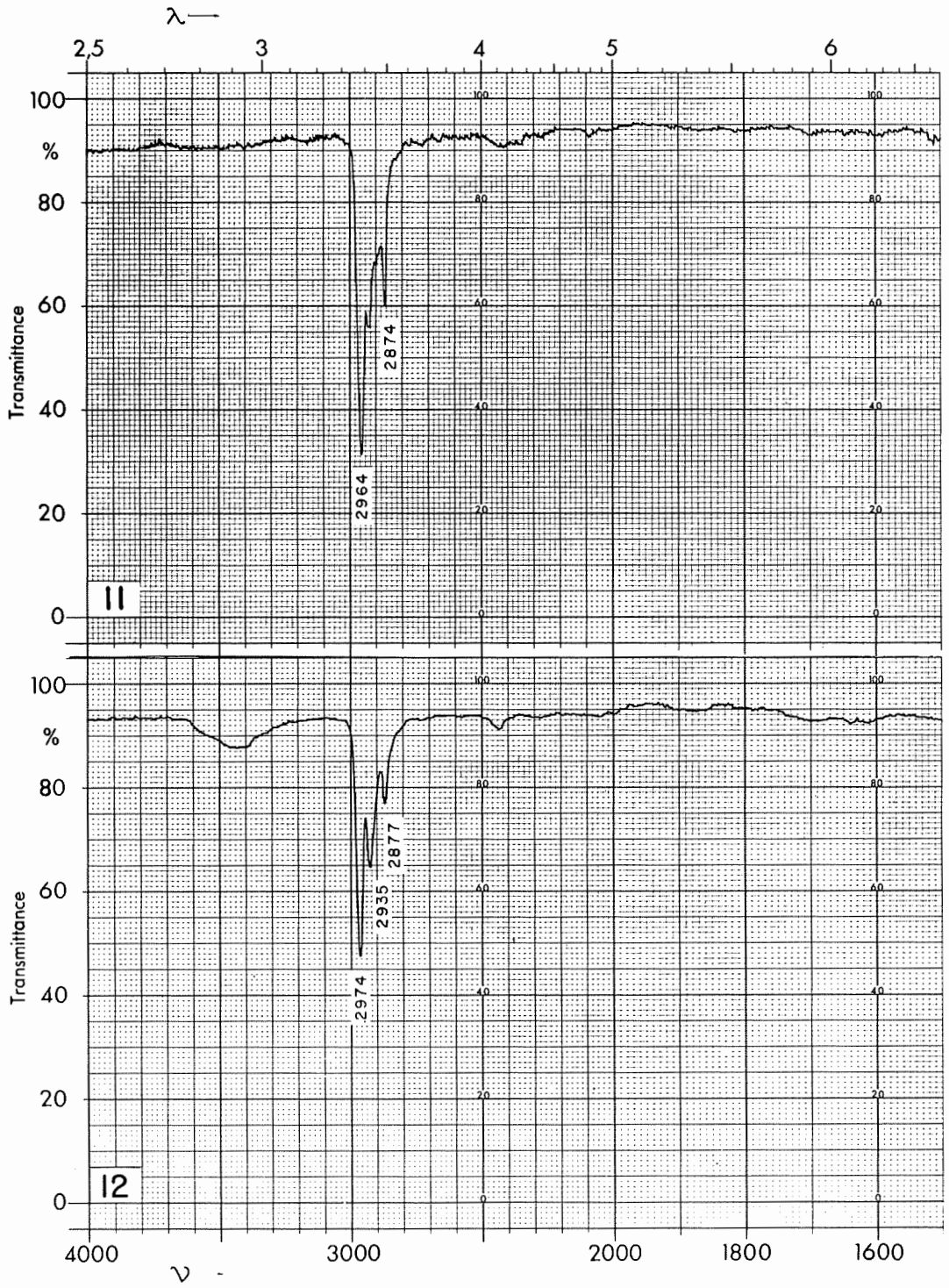

FIGURE 10. - Spectra of (11) zinc isobutyl xanthate and (12) zinc secondary-butyl xanthate.

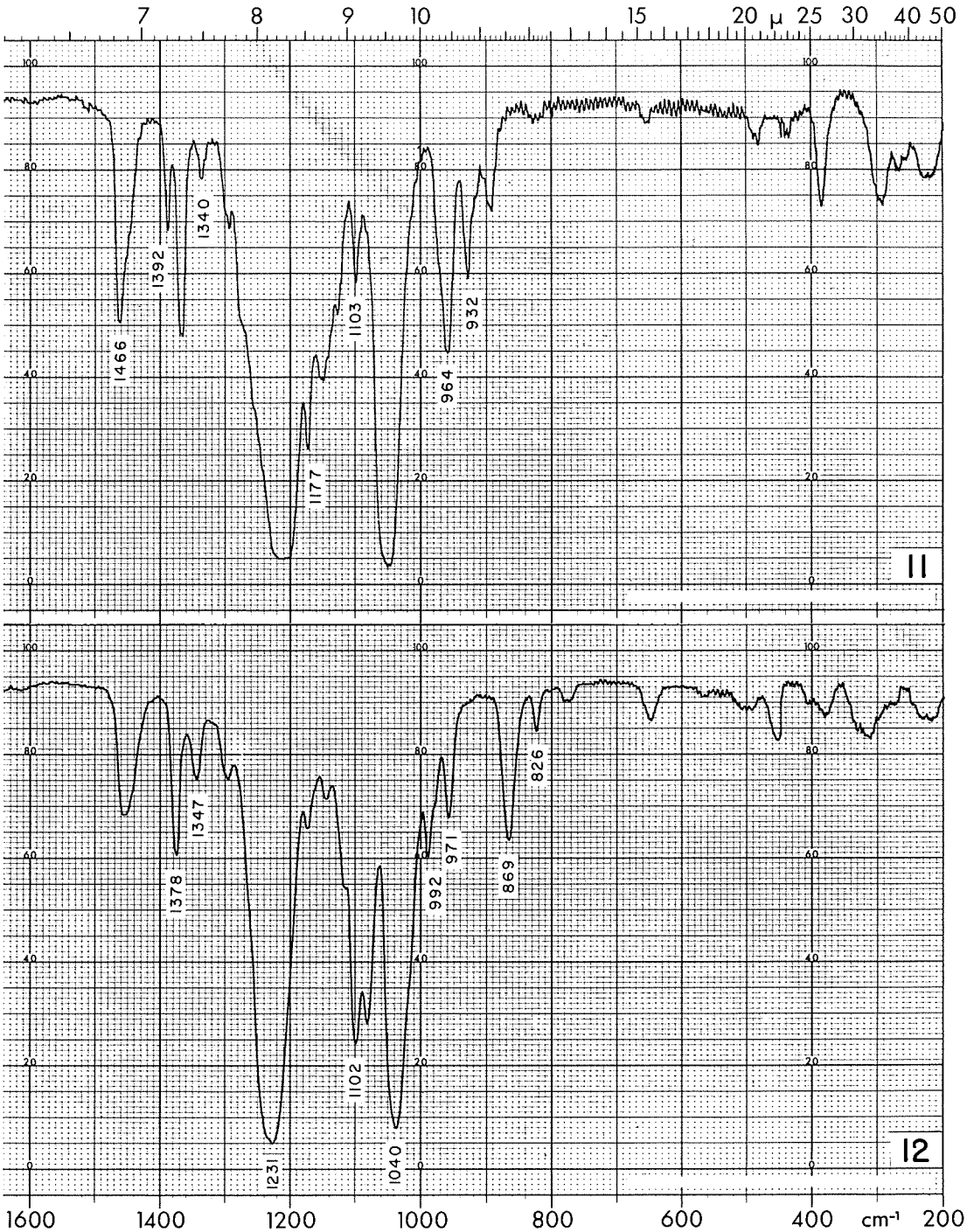

FIGURE 10. - Spectra of (11) zinc isobutyl xanthate and (12) zinc secondary-butyl xanthate.–Continued

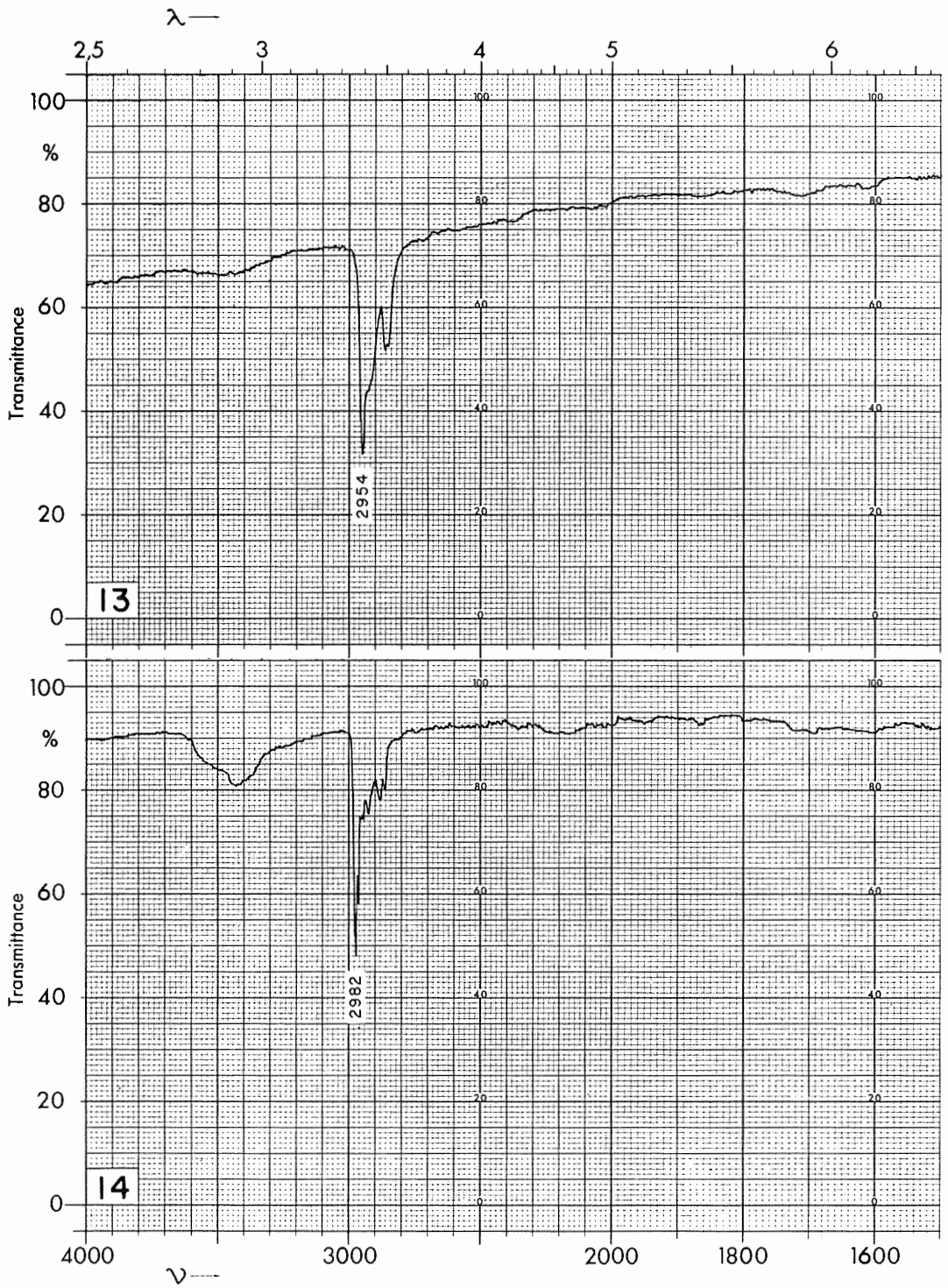

FIGURE 11. - Spectra of (13) zinc n-amyl xanthate and (14) potassium ethyl xanthate.

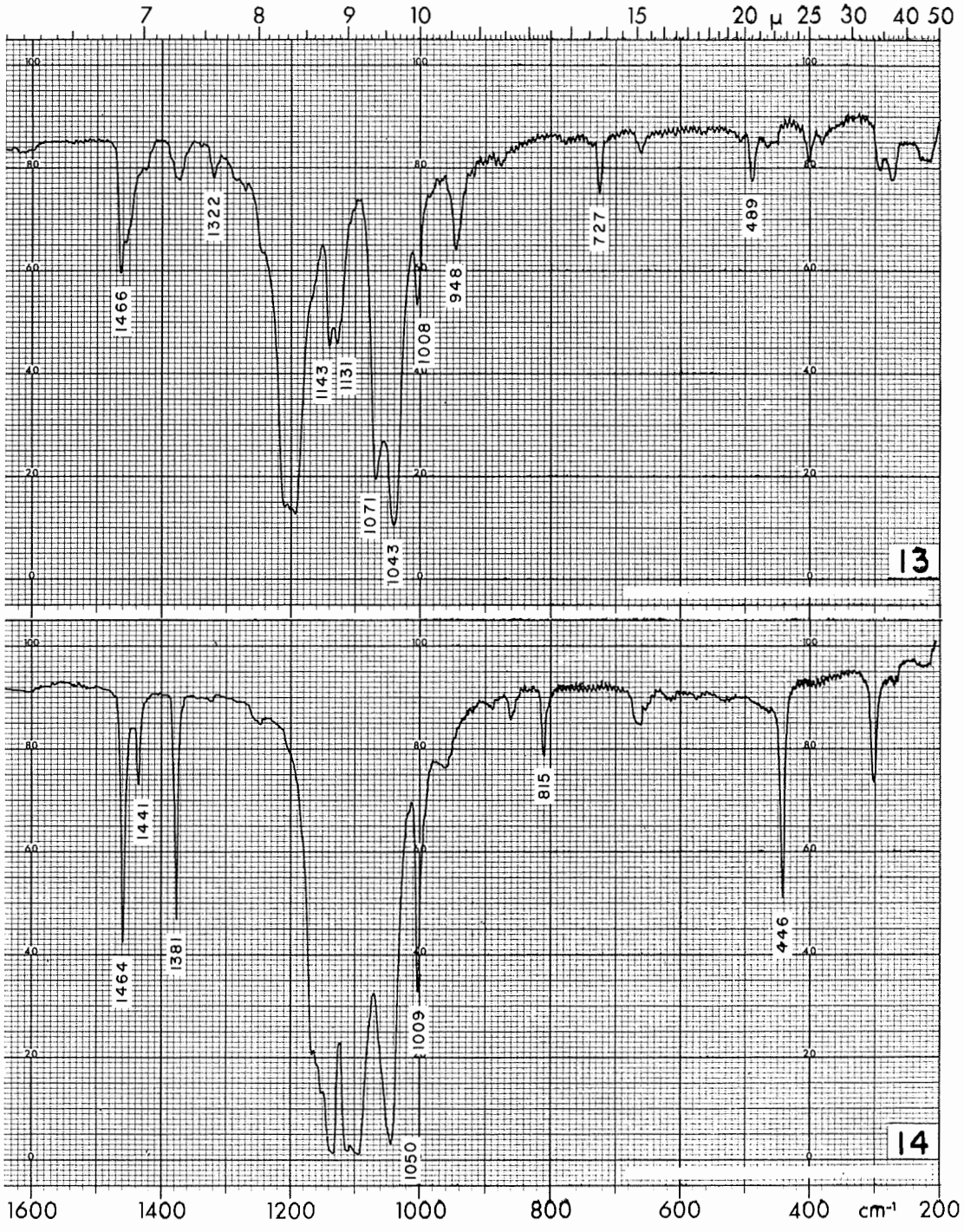

FIGURE 11. - Spectra of (13) zinc n-amyl xanthate and (14) potassium ethyl xanthate.–Continued

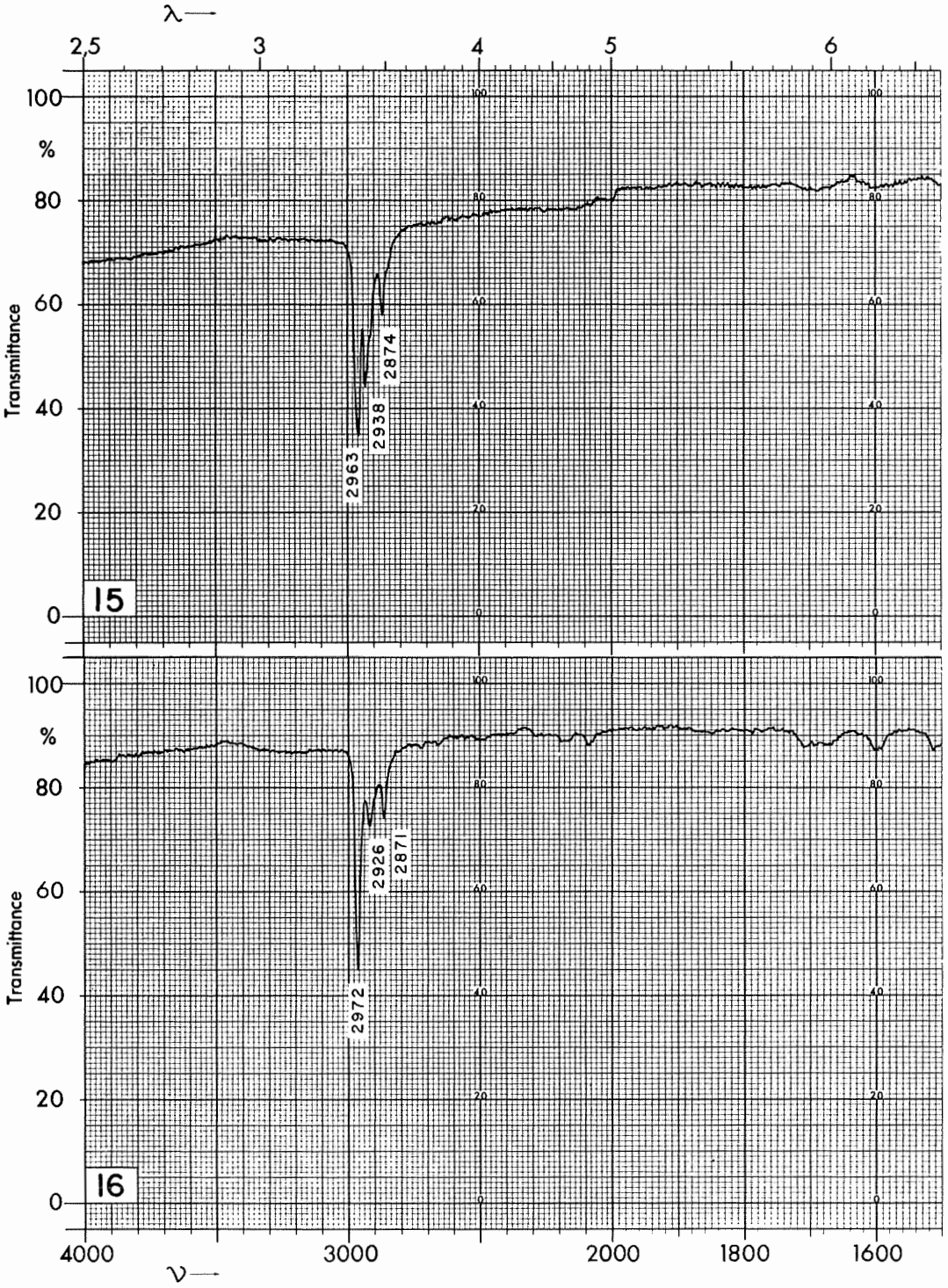

FIGURE 12. - Spectra of (15) potassium n-propyl xanthate and (16) potassium isopropyl xanthate.

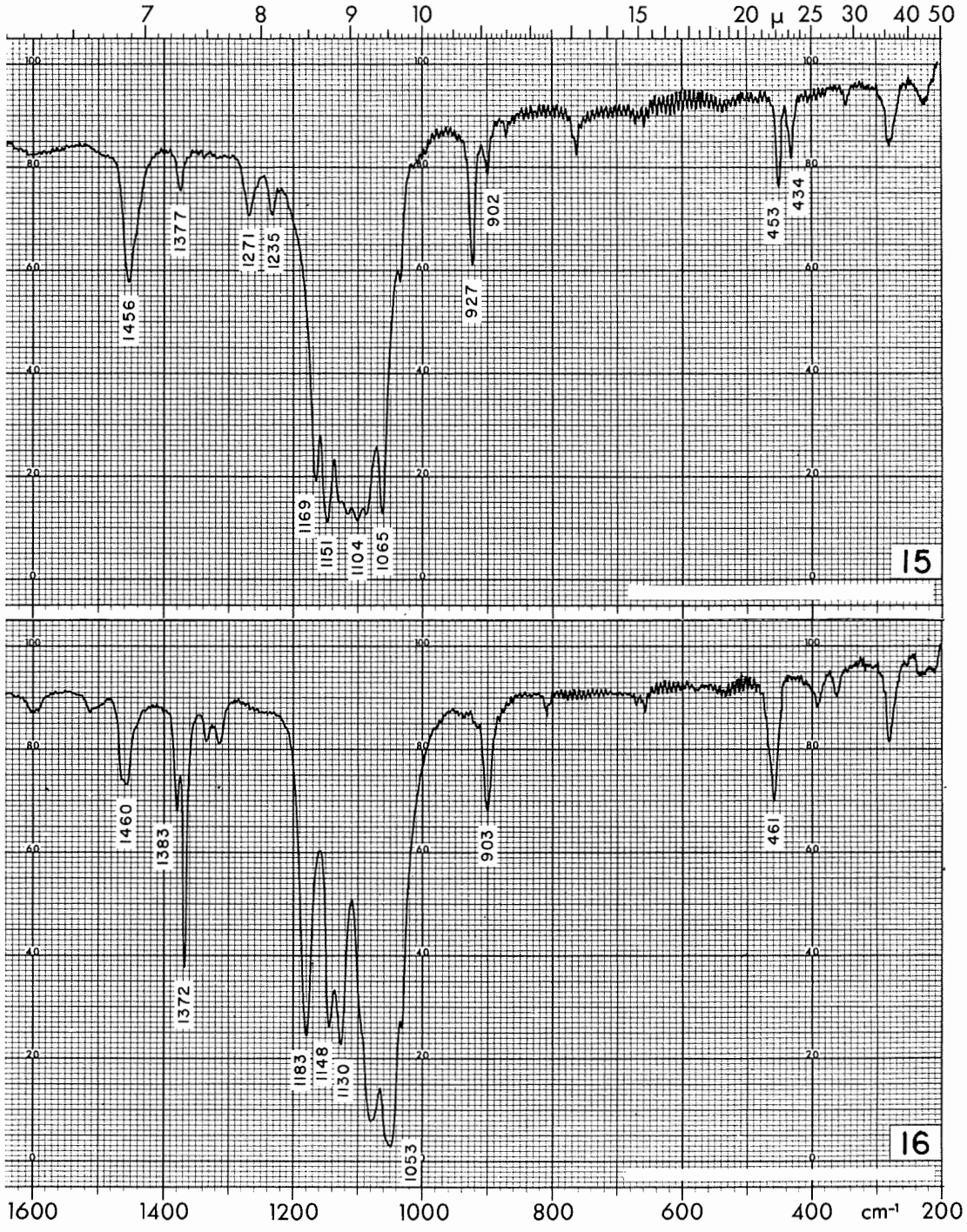

FIGURE 12. - Spectra of (15) potassium n-propyl xanthate and (16) potassium isopropyl xanthate.—Continued

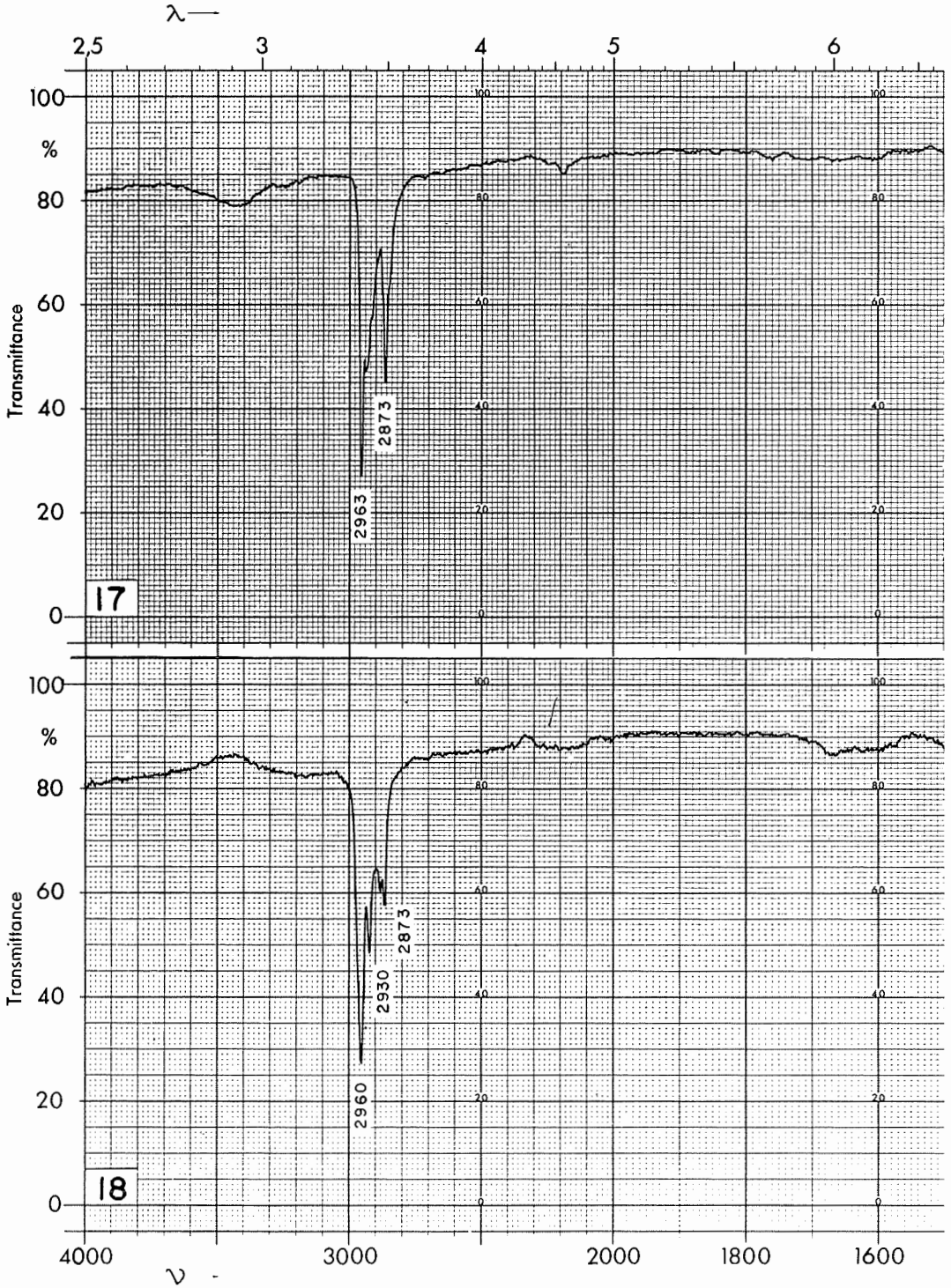

FIGURE 13. - Spectra of (17) potassium n-butyl xanthate and (18) potassium isobutyl xanthate.

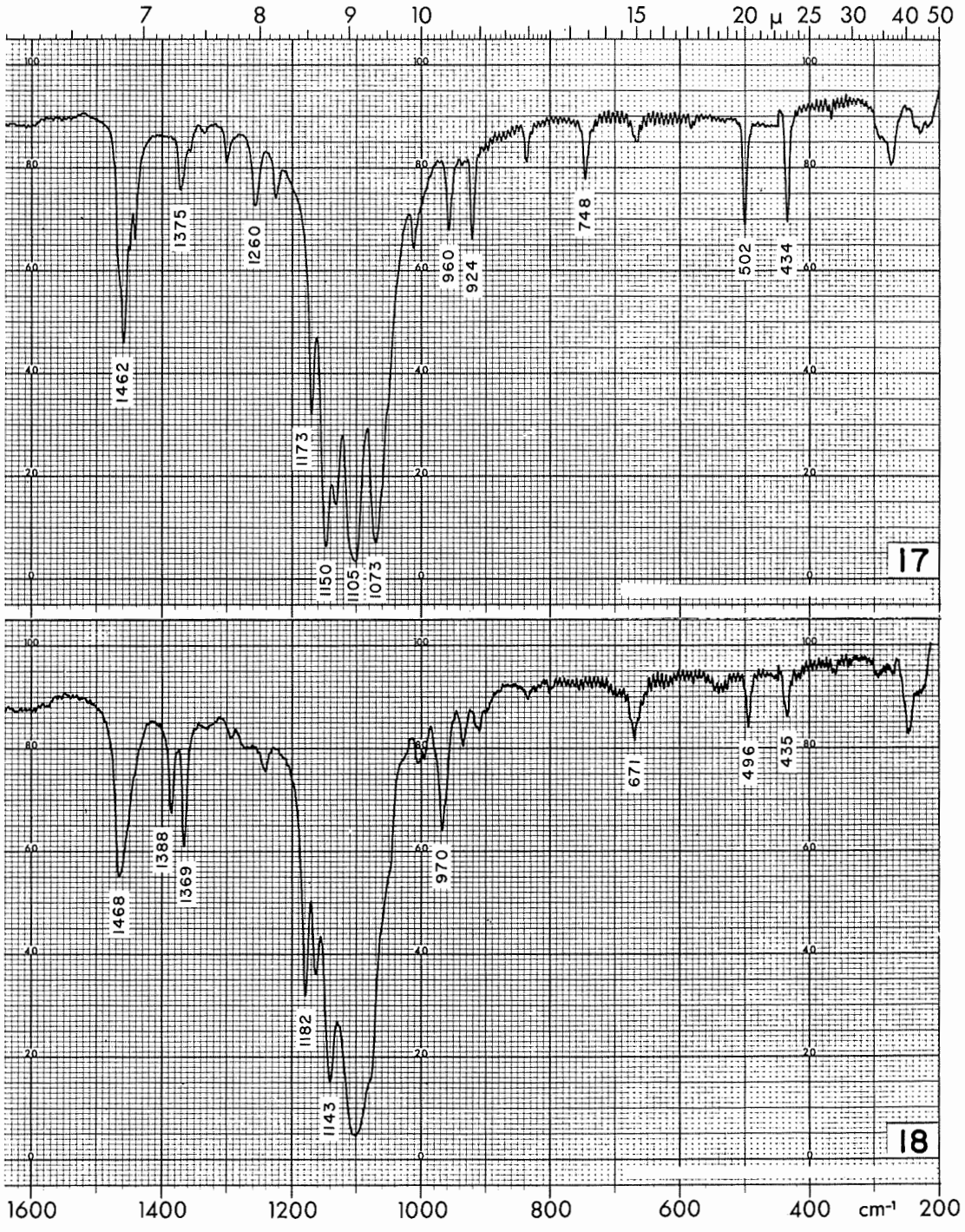

FIGURE 13. - Spectra of (17) potassium n-butyl xanthate and (18) potassium isobutyl xanthate.–Continued

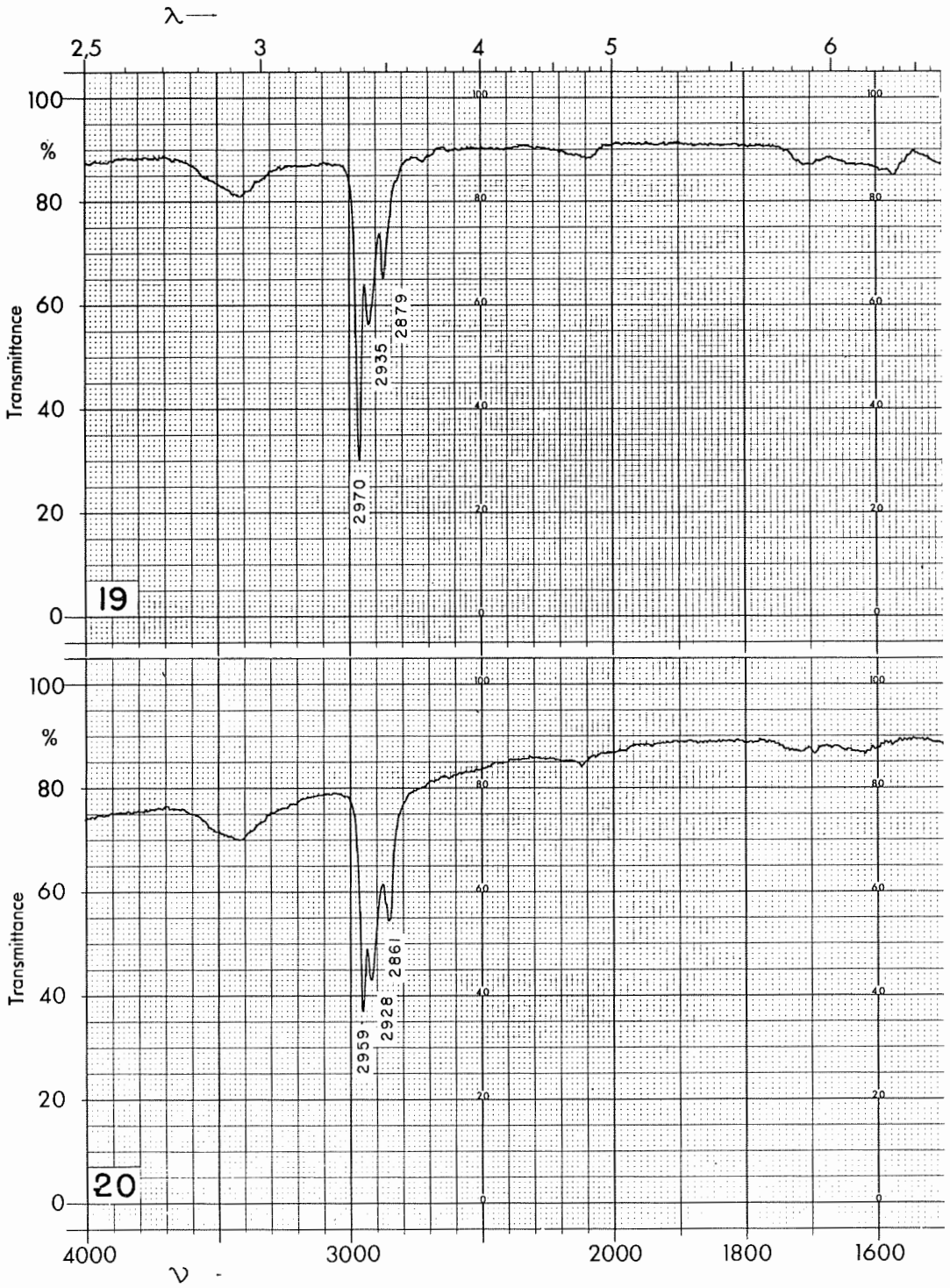

FIGURE 14. - Spectra of (19) potassium secondary-butyl xanthate and (20) potassium n-amyl xanthate.

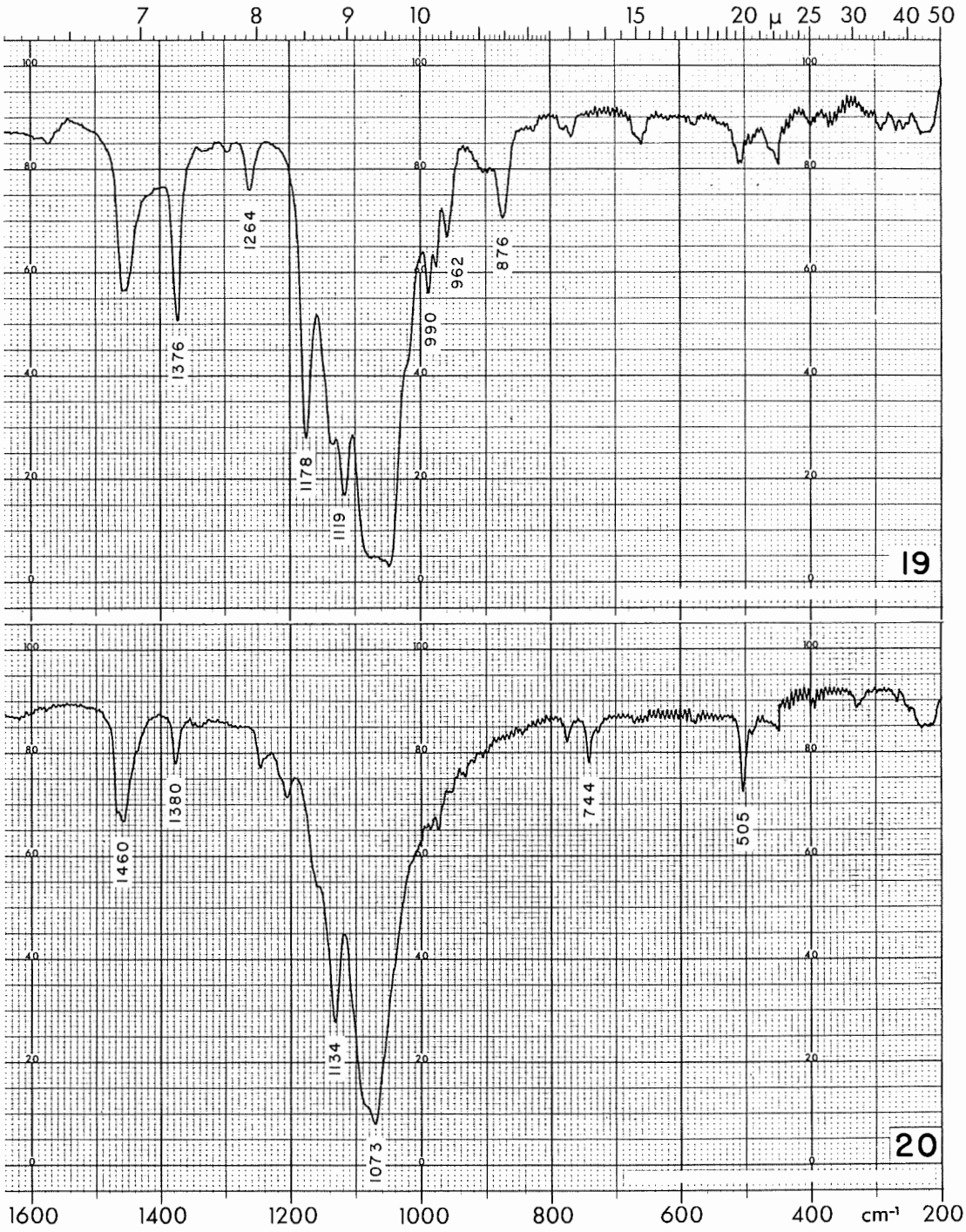

FIGURE 14. - Spectra of (19) potassium secondary-butyl xanthate and (20) potassium n-amyl xanthate.–Continued

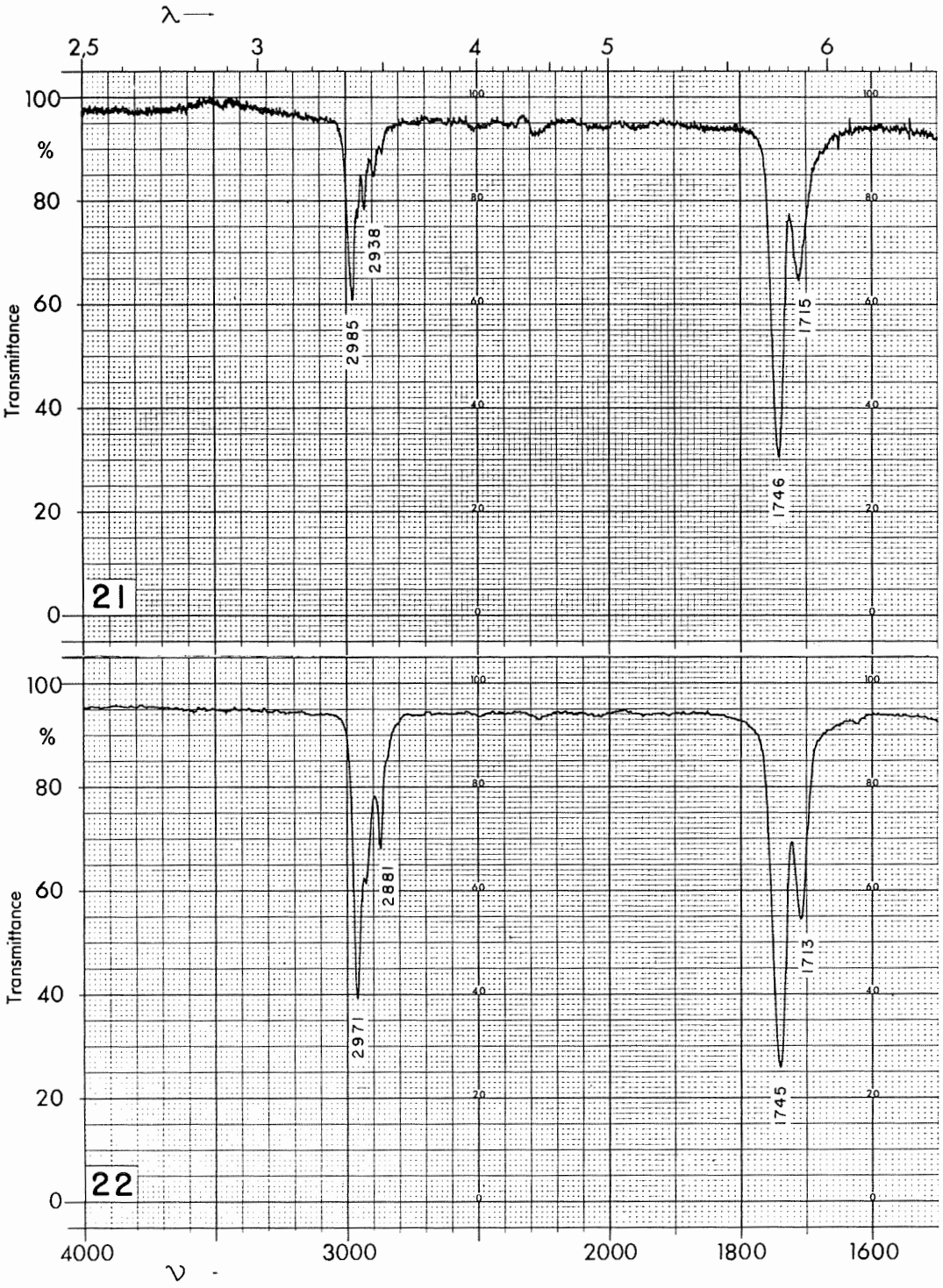

FIGURE 15. - Spectra of (21) di-ethyl dixanthogen and (22) di-n-propyl dixanthogen.

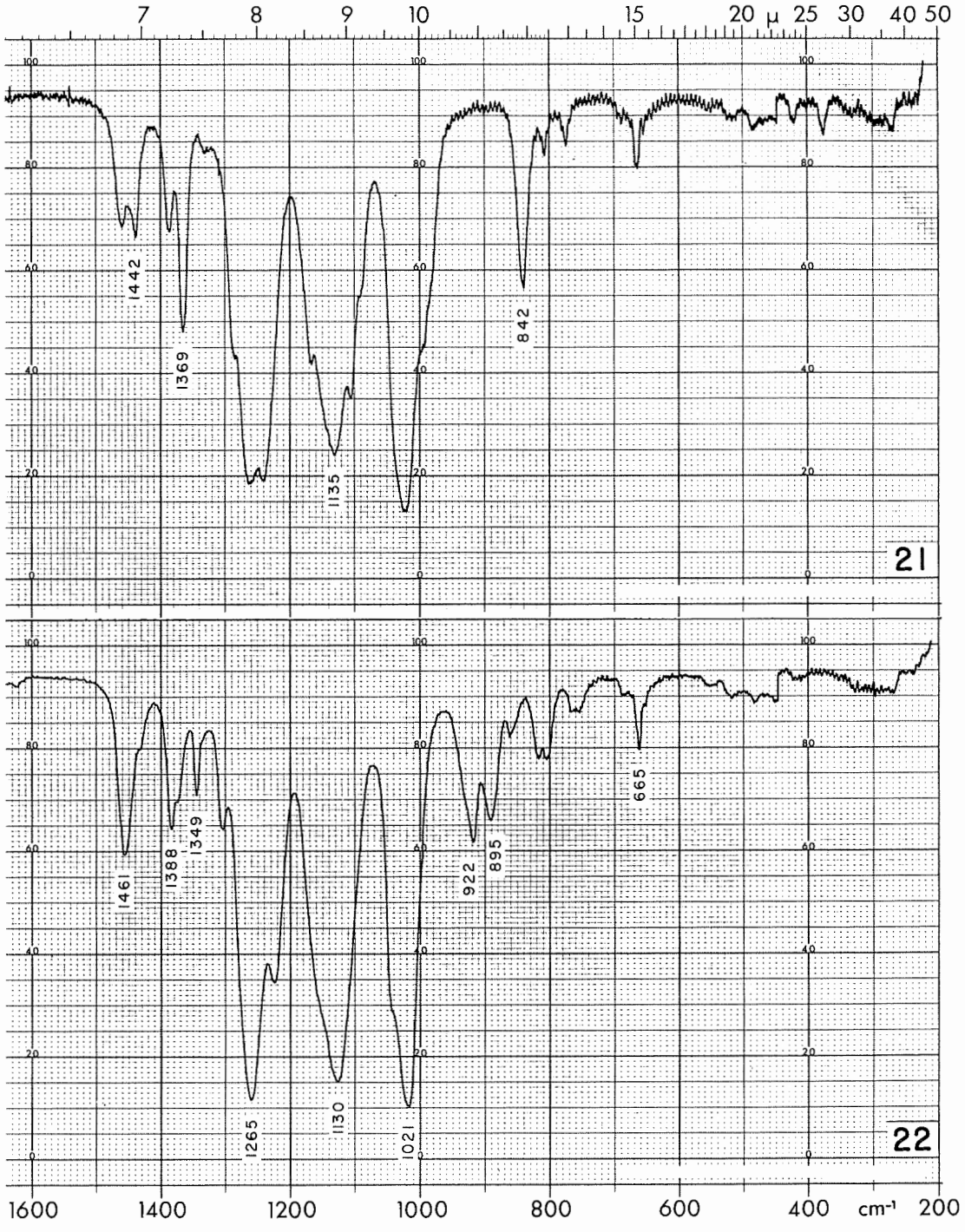

FIGURE 15. - Spectra of (21) di-ethyl dixanthogen and (22) di-n-propyl dixanthogen.—Continued

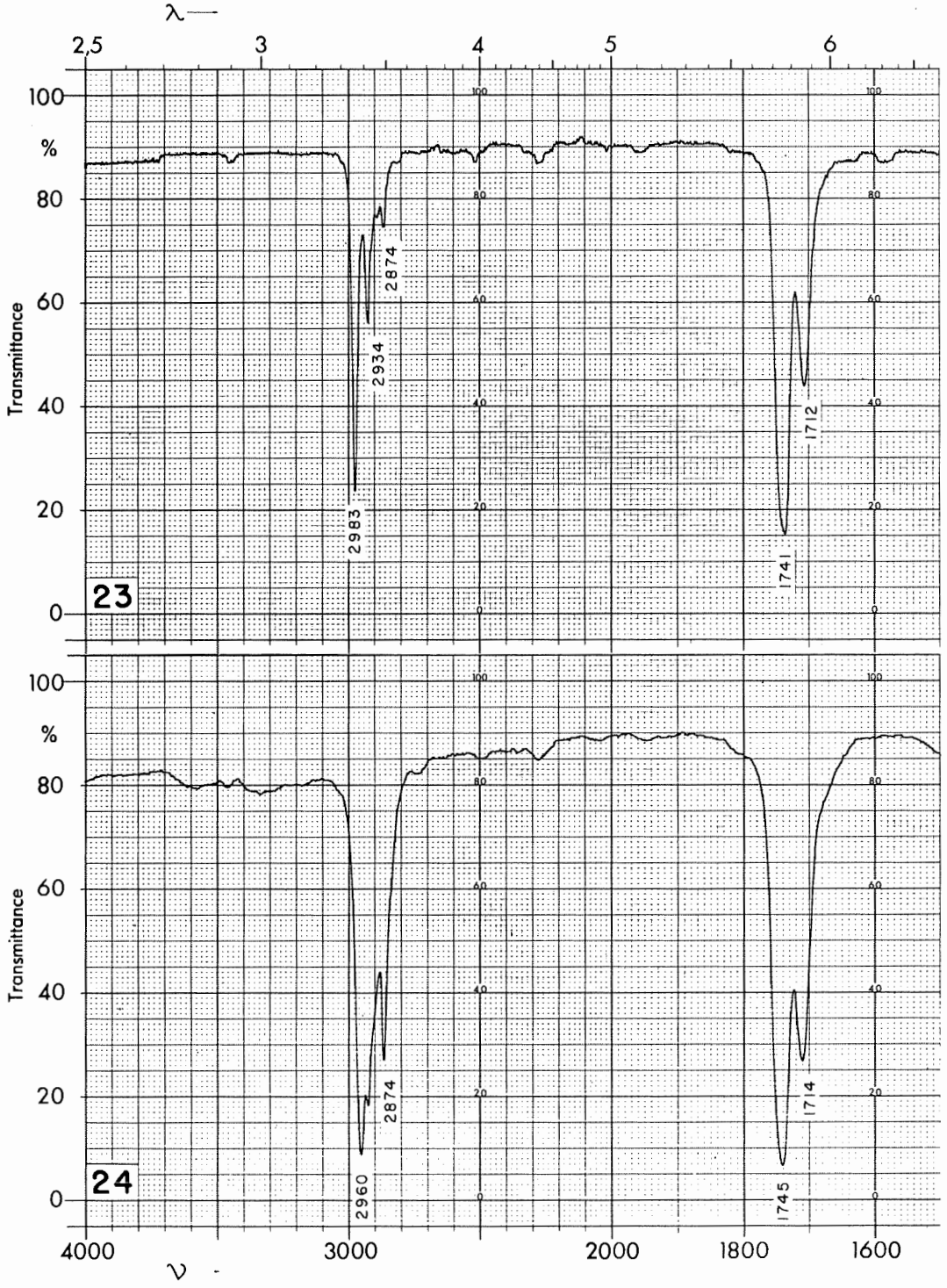

FIGURE 16. - Spectra of (23) di-isopropyl dixanthogen and (24) di-n-butyl dixanthogen.

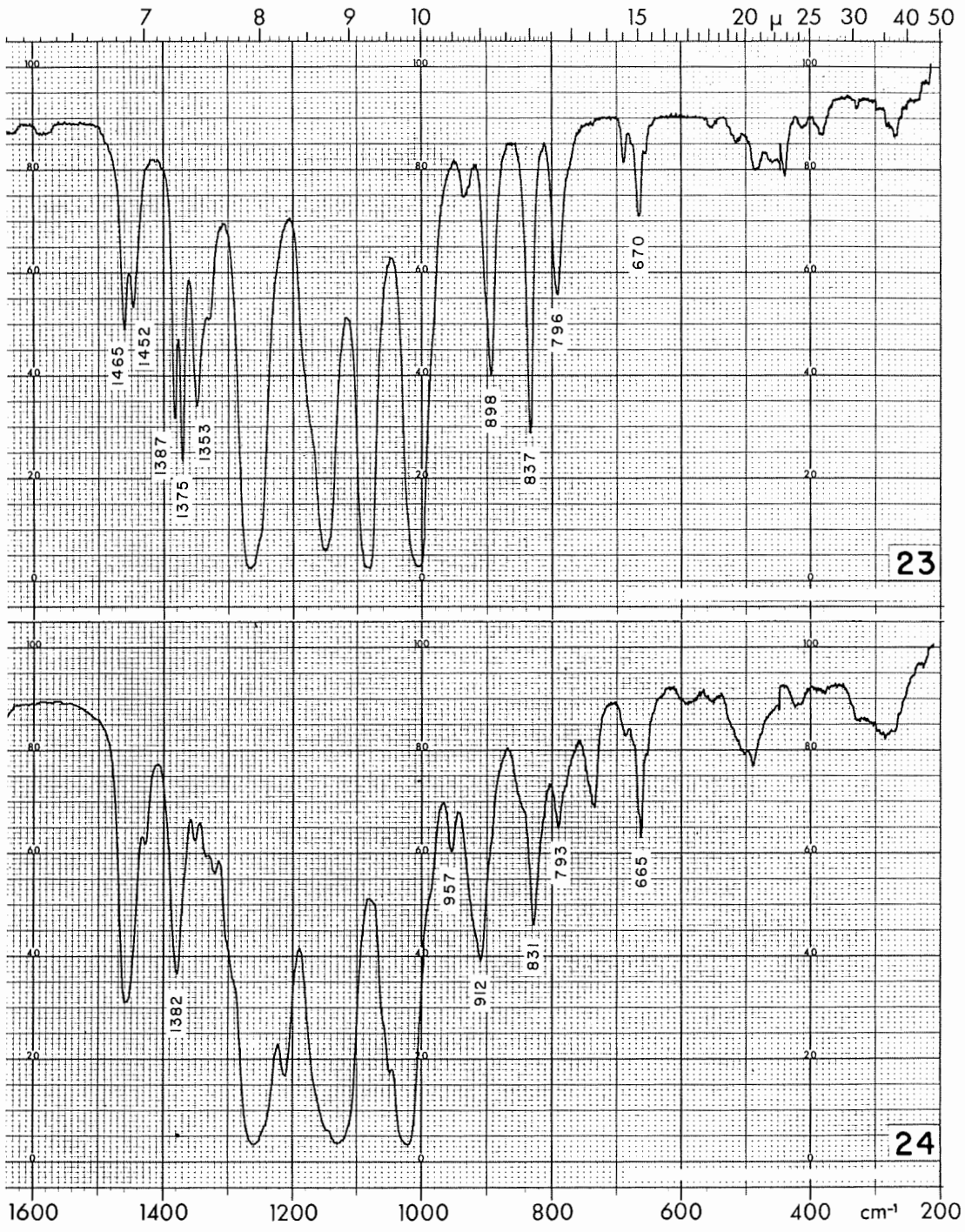

FIGURE 16. - Spectra of (23) di-isopropyl dixanthogen and (24) di-n-butyl dixanthogen.–Continued

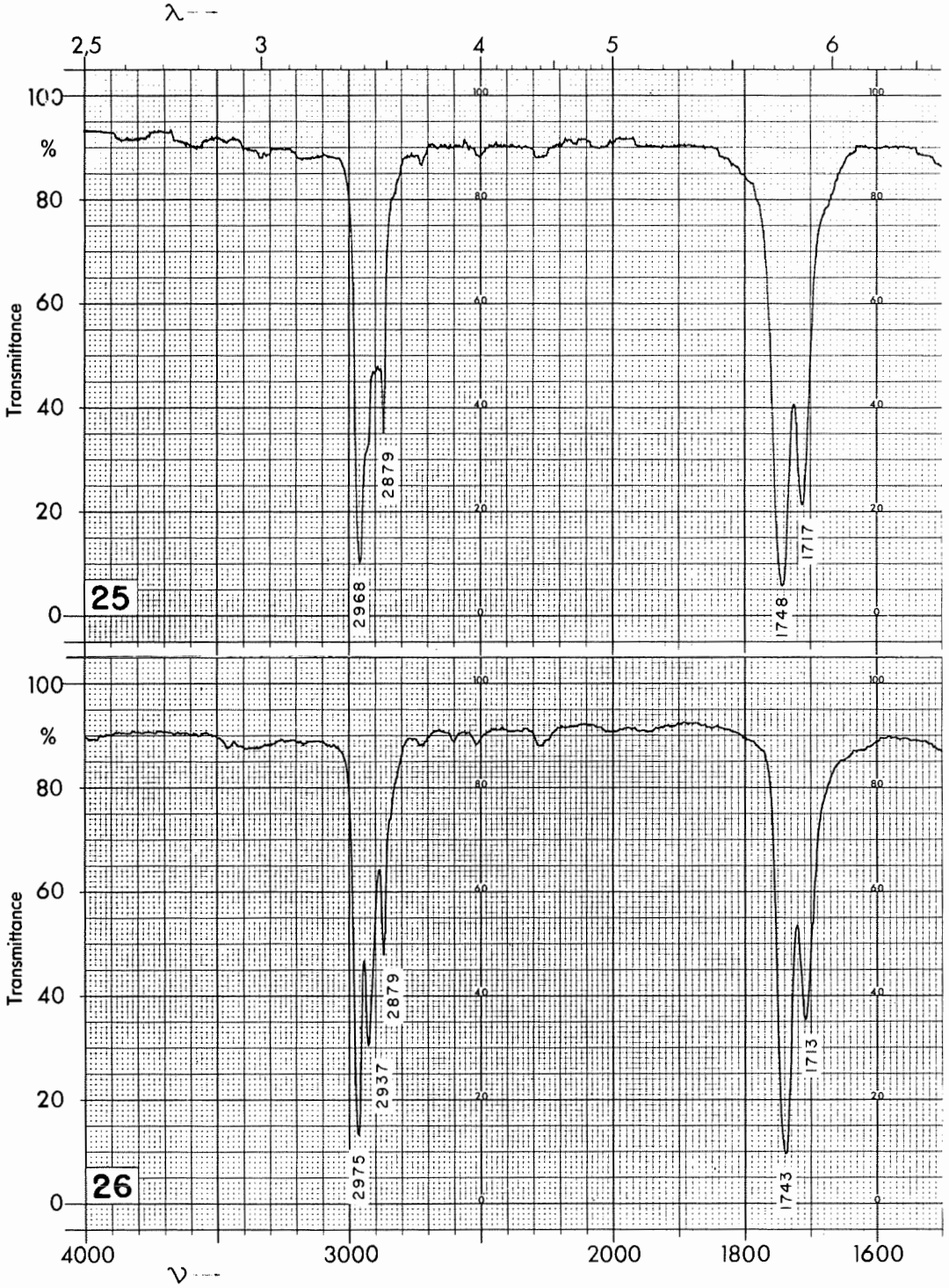

FIGURE 17. - Spectra of (25) di-isobutyl dixanthogen and (26) di-secondary-butyl dixanthogen.

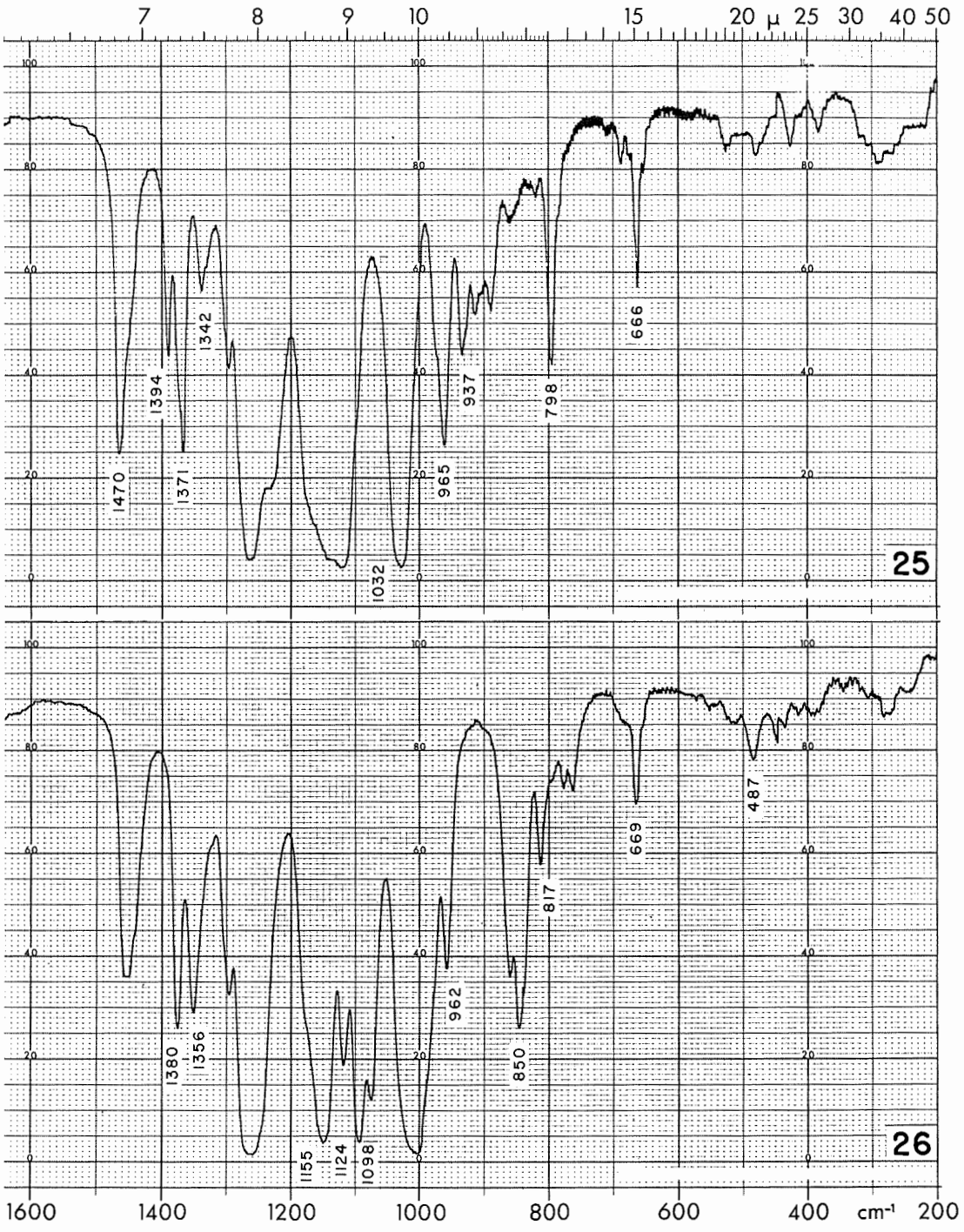

FIGURE 17. - Spectra of (25) di-isobutyl dixanthogen and (26) di-secondary-butyl dixanthogen.—Continued

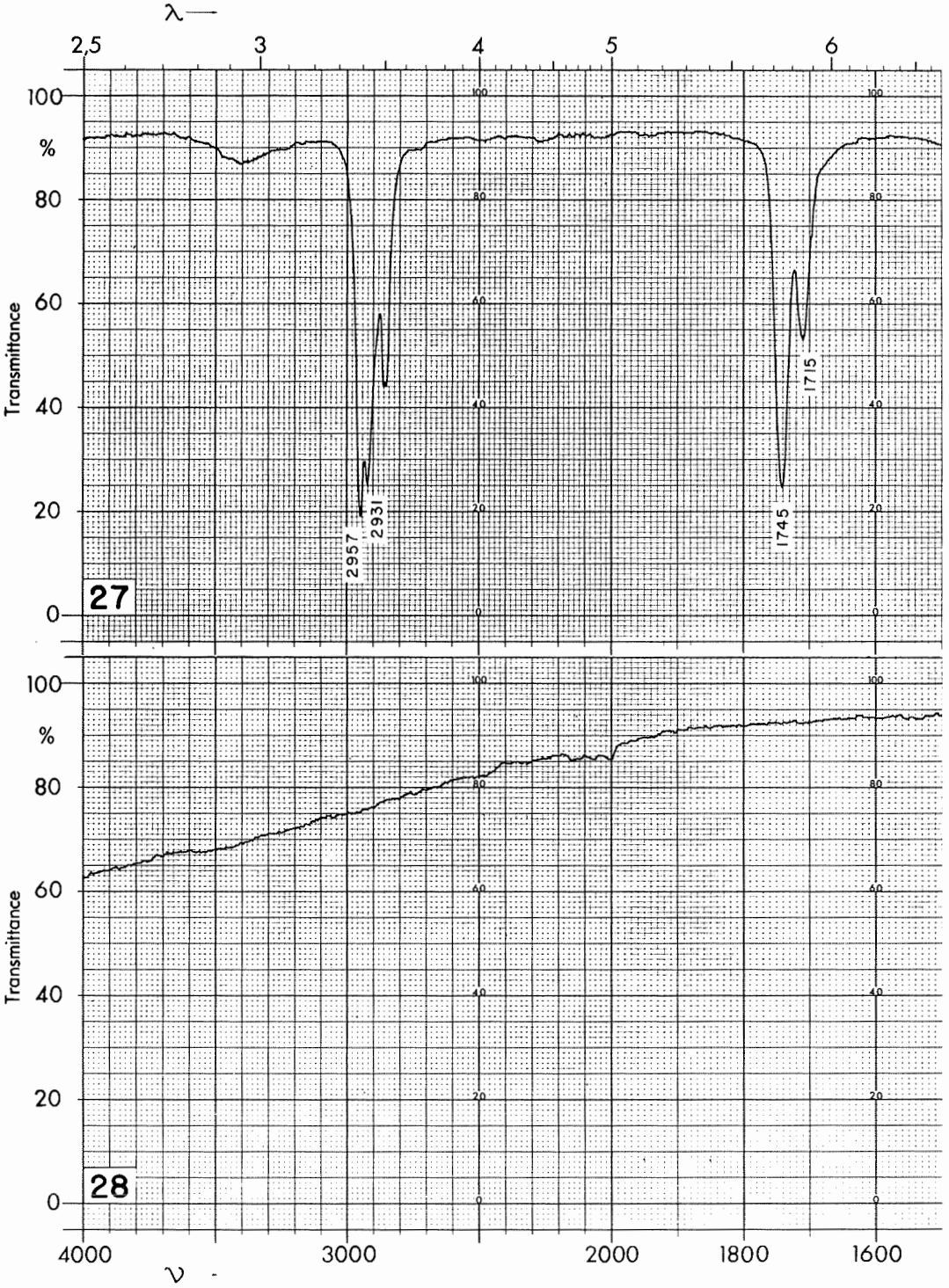

FIGURE 18. - Spectra of (27) di-n-amyl dixanthogen and (28) lead sulfate.

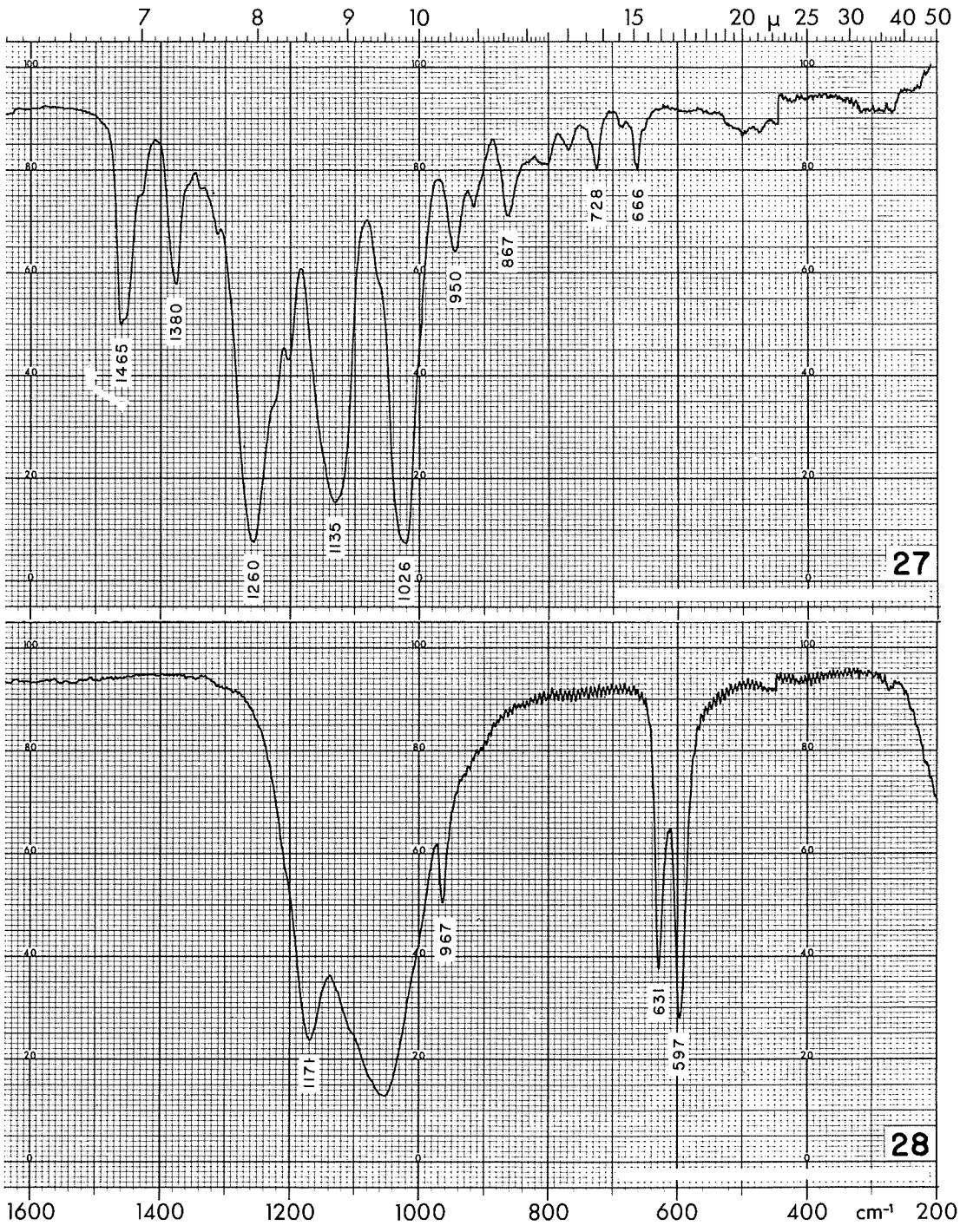

FIGURE 18. - Spectra of (27) di-n-amyl dixanthogen and (28) lead sulfate.—Continued

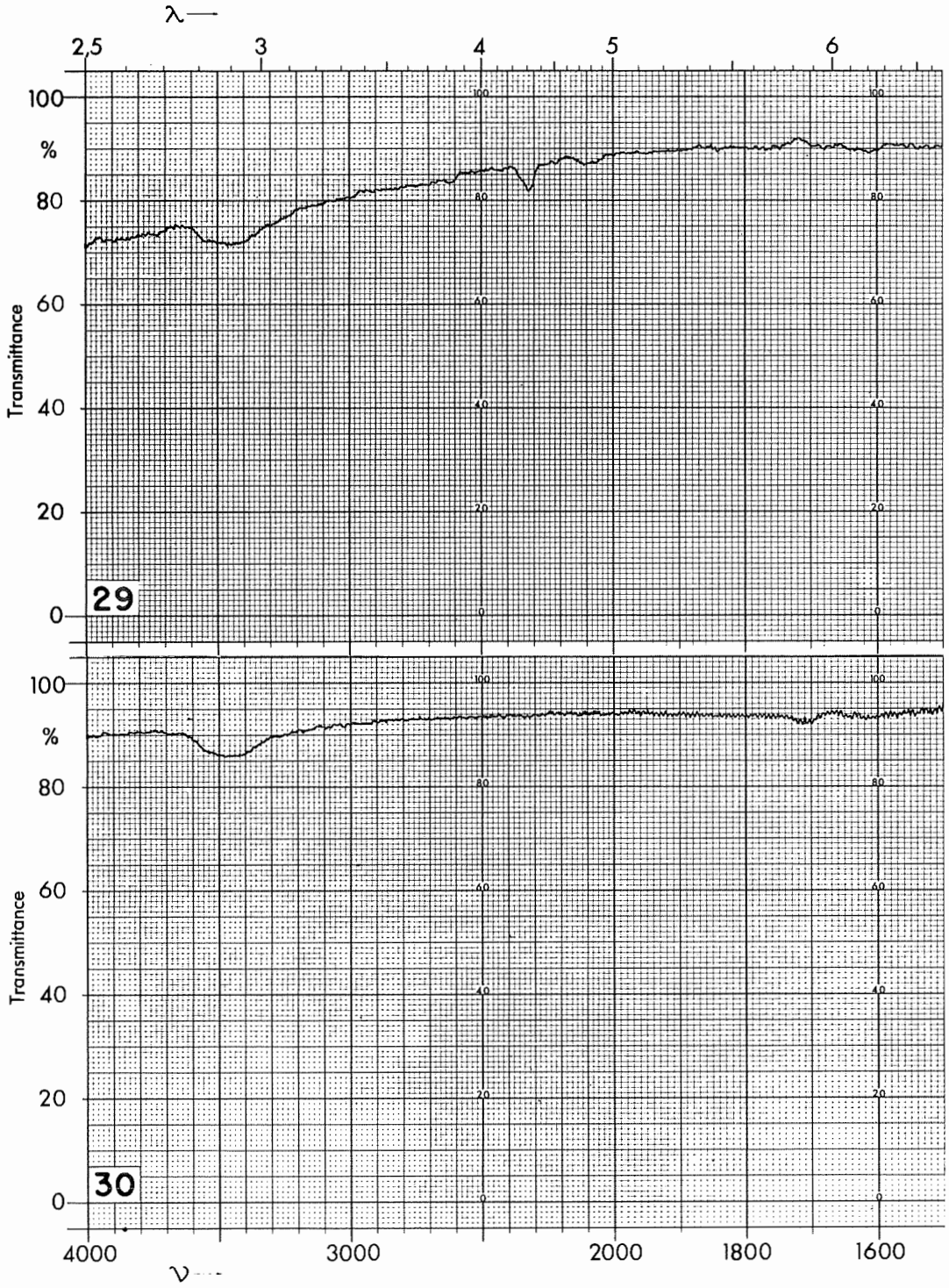

FIGURE 19. - Spectra of (29) lead thiosulfate and (30) lead sulfite.

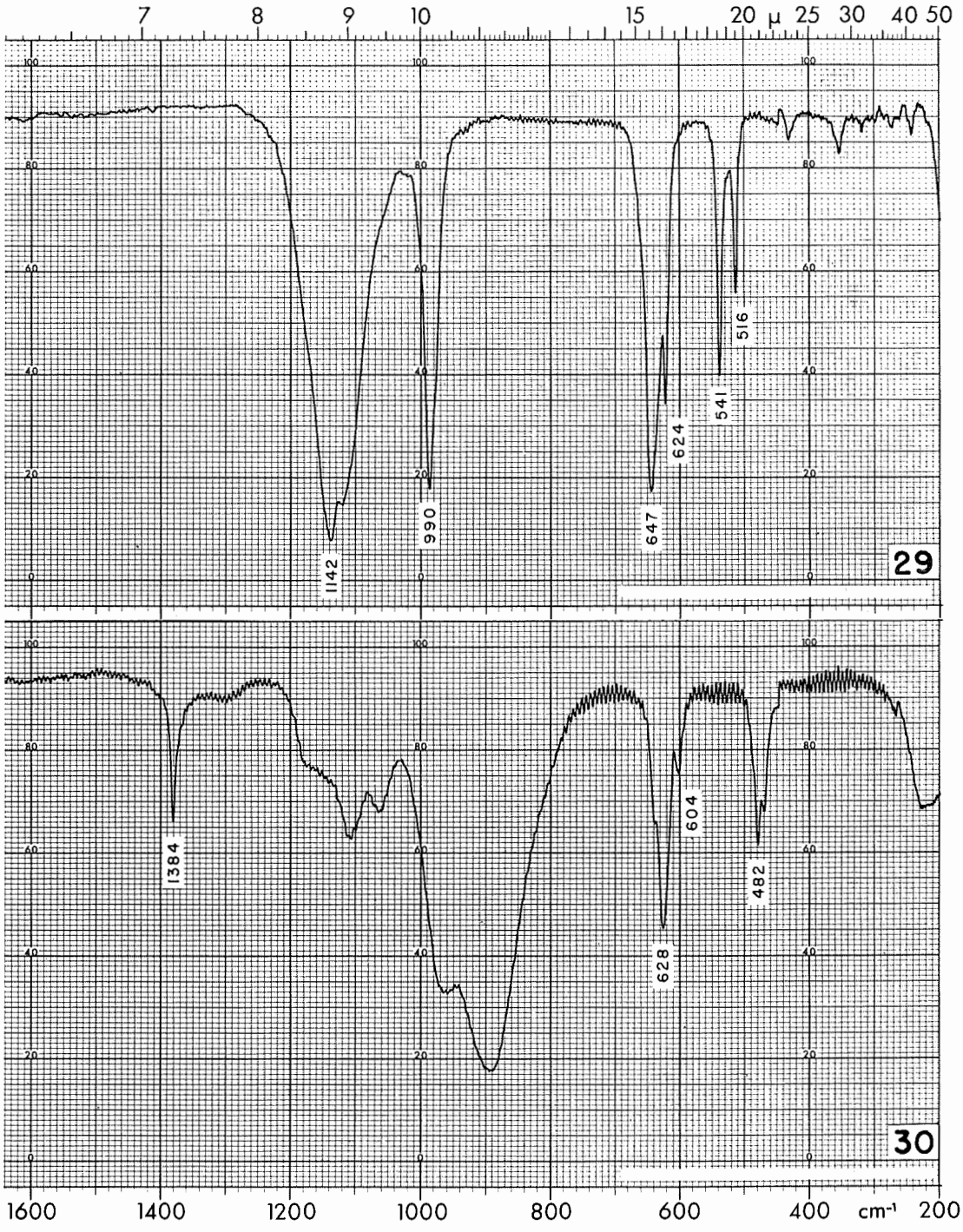

FIGURE 19. - Spectra of (29) lead thiosulfate and (30) lead sulfite.–Continued

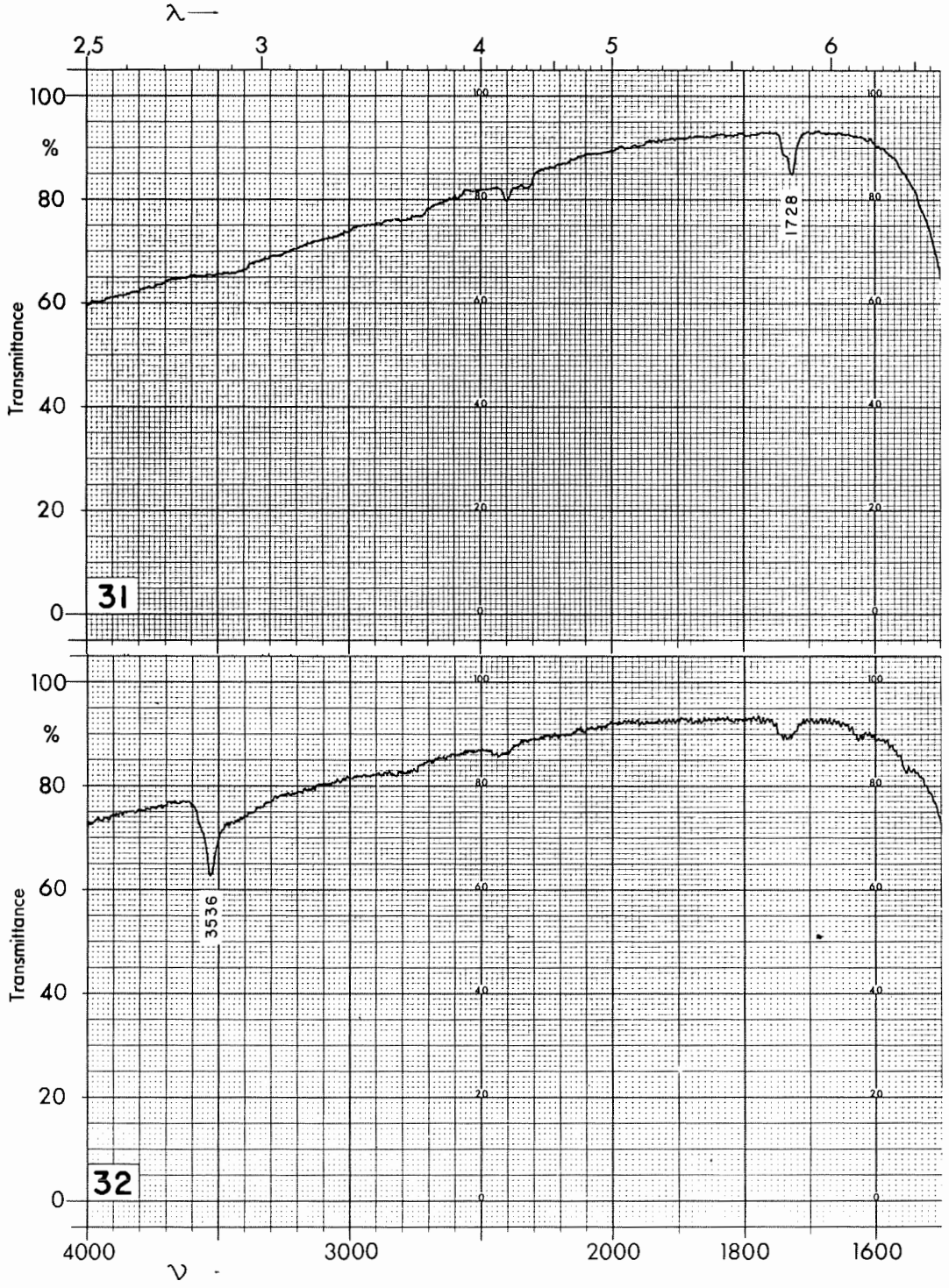

FIGURE 20. - Spectra of (31) lead carbonate and (32) basic lead carbonate.

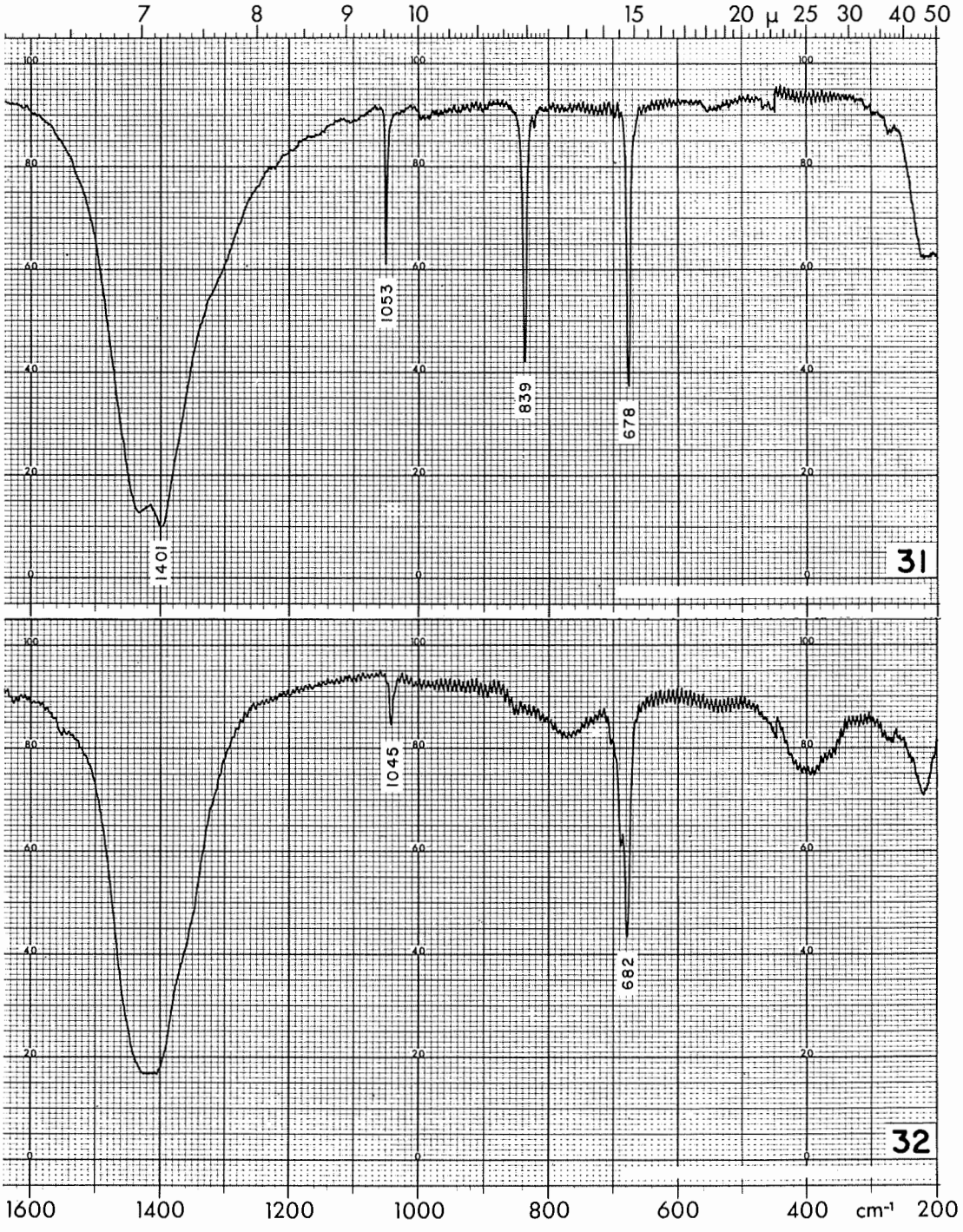

FIGURE 20. - Spectra of (31) lead carbonate and (32) basic lead carbonate.—Continued

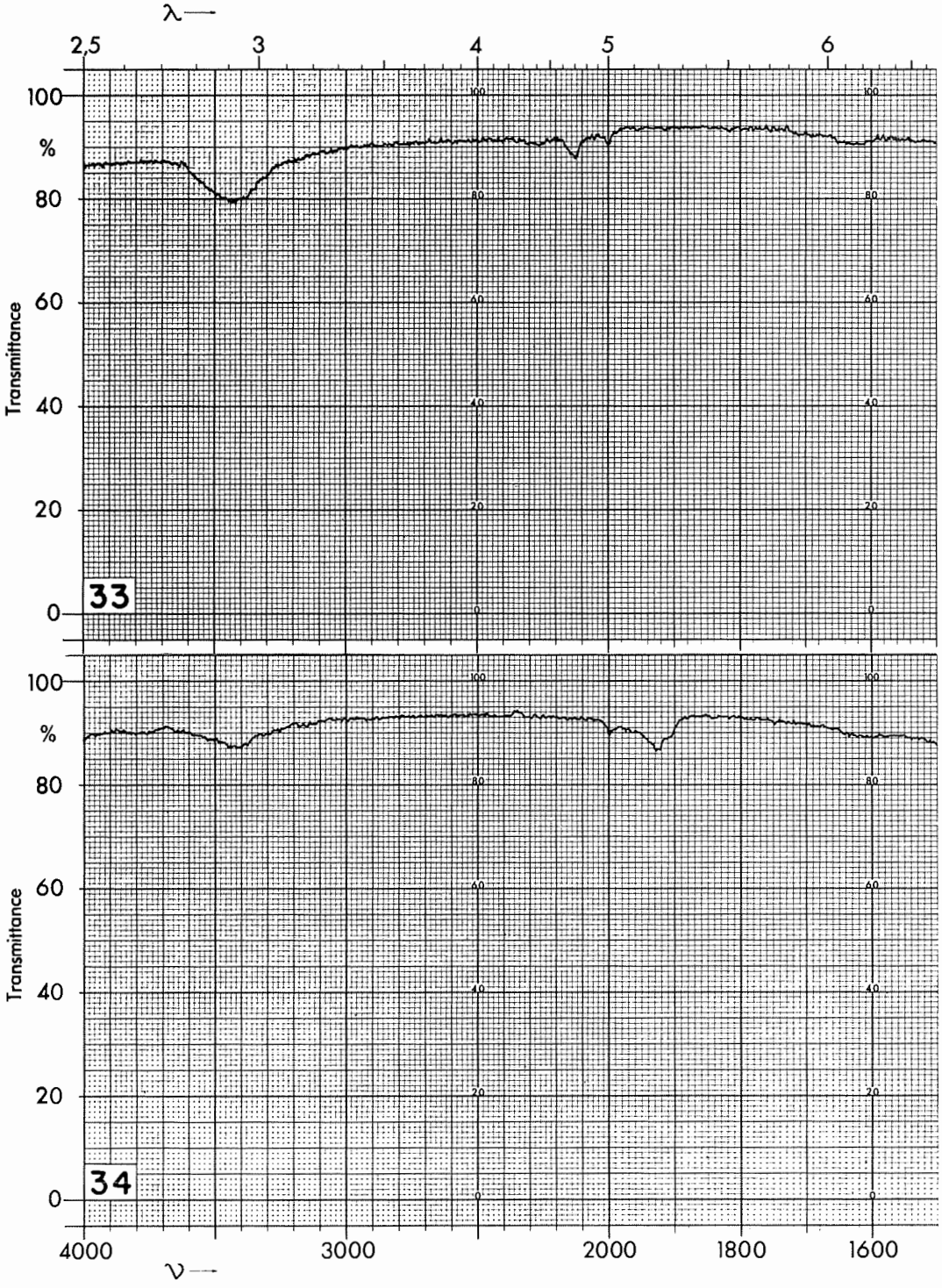

FIGURE 21. - Spectra of (33) sodium thiosulfate and (34) sodium sulfite.

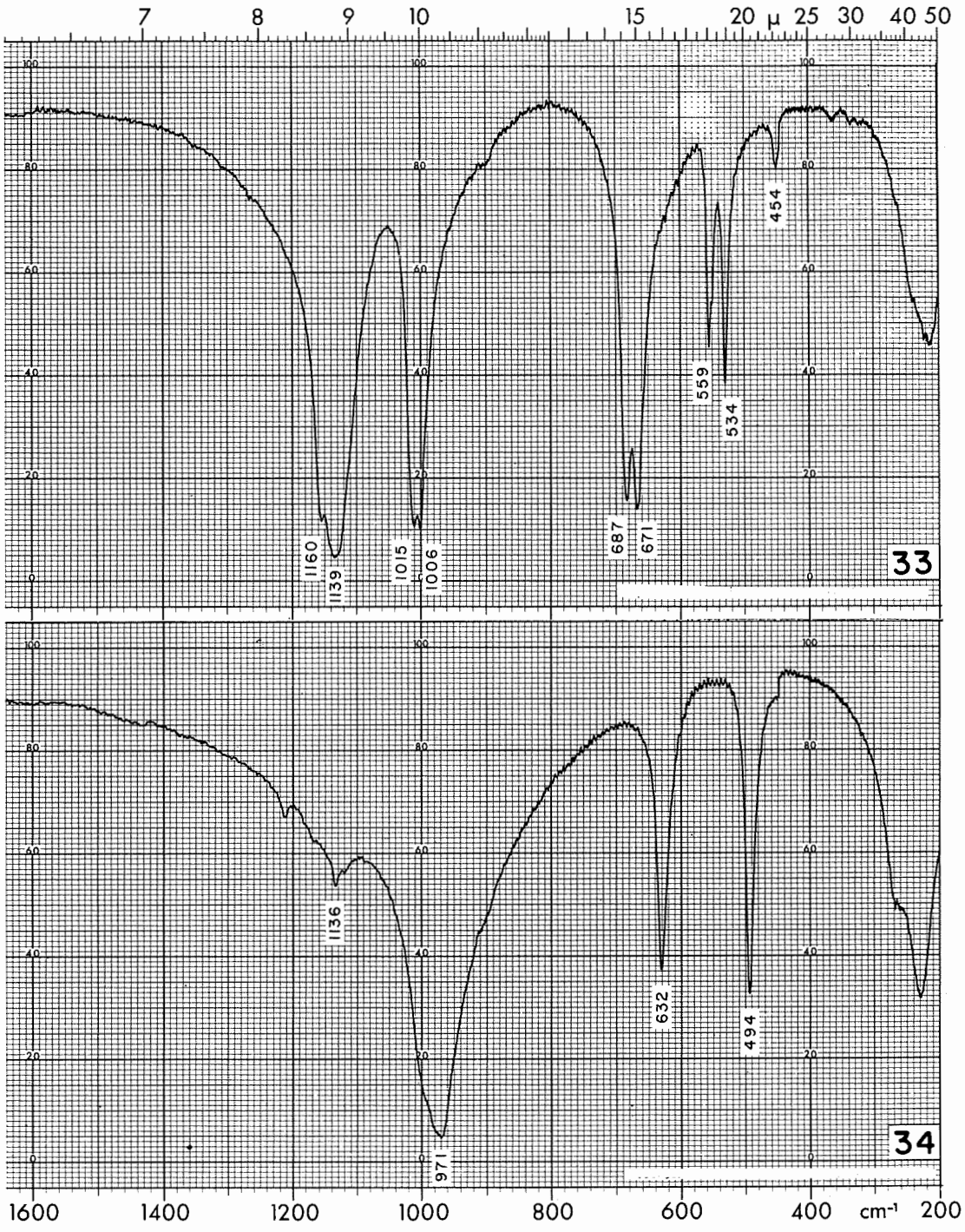

FIGURE 21. - Spectra of (33) sodium thiosulfate and (34) sodium sulfite.–Continued

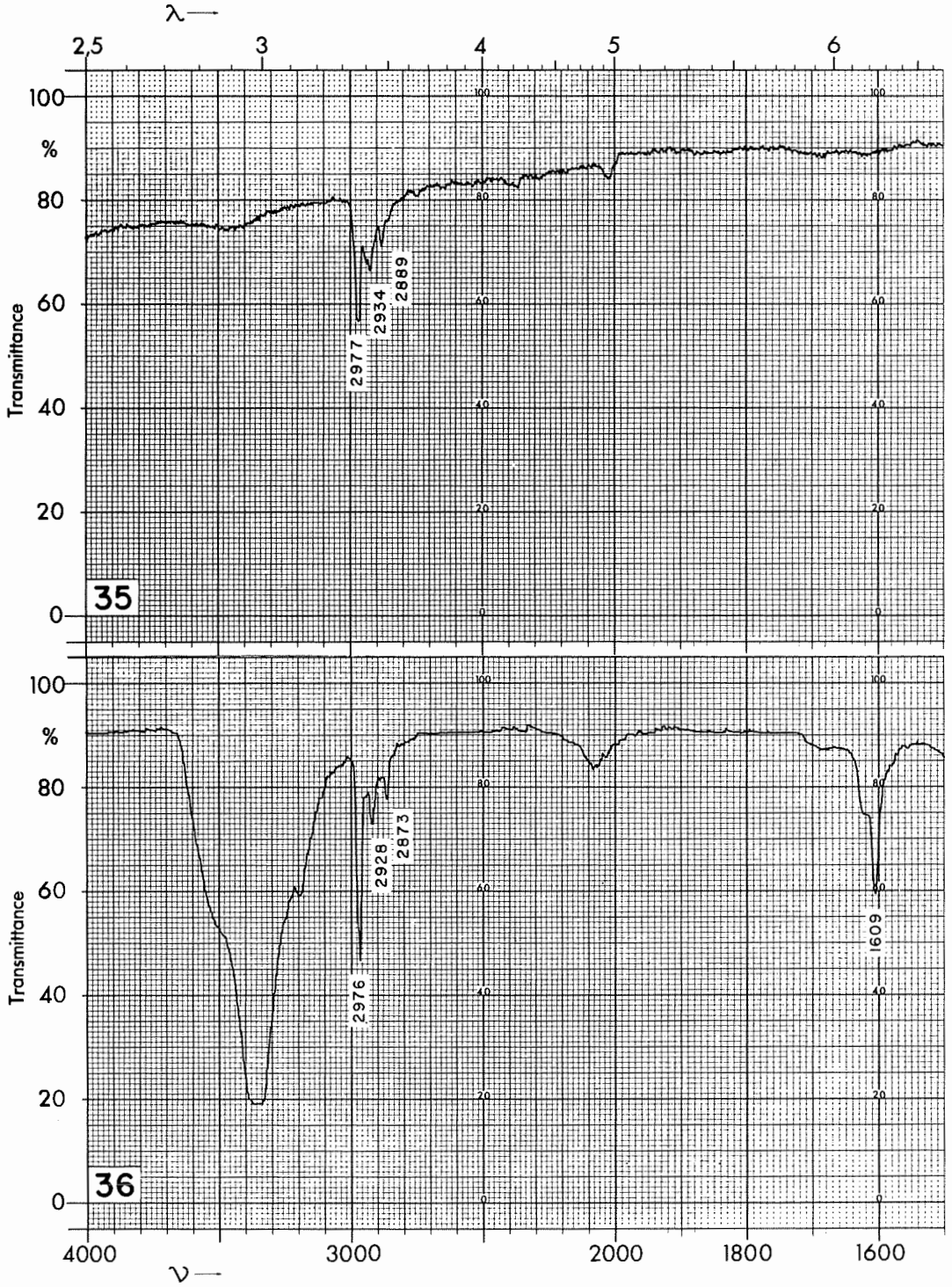

FIGURE 22. - Spectra of (35) cuprous ethyl xanthate and (36) commercial flotation reagent sodium isopropyl xanthate (Dow Z-11).

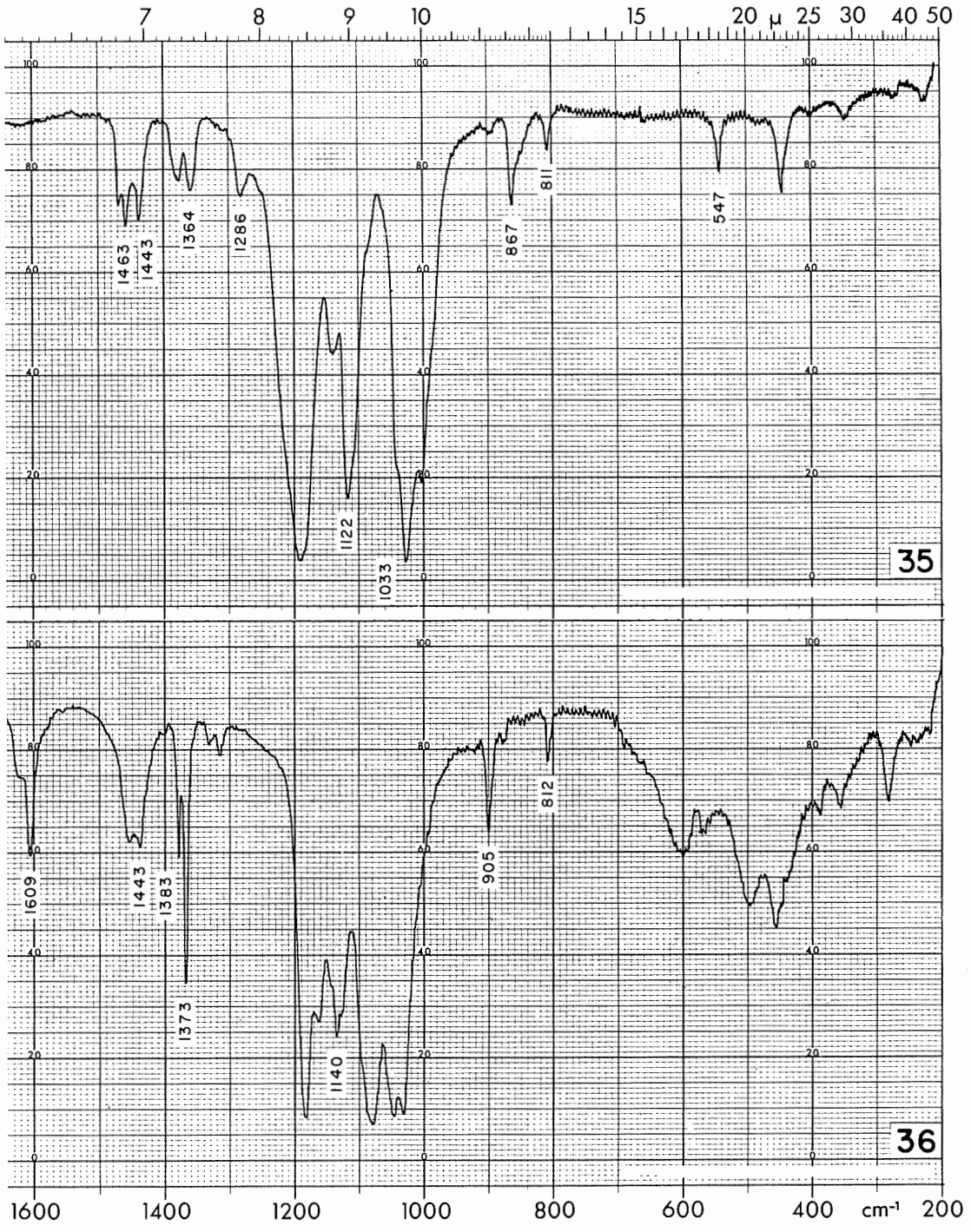

FIGURE 22. - Spectra of (35) cuprous ethyl xanthate and (36) commercial flotation reagent sodium isopropyl xanthate (Dow Z-11).–Continued

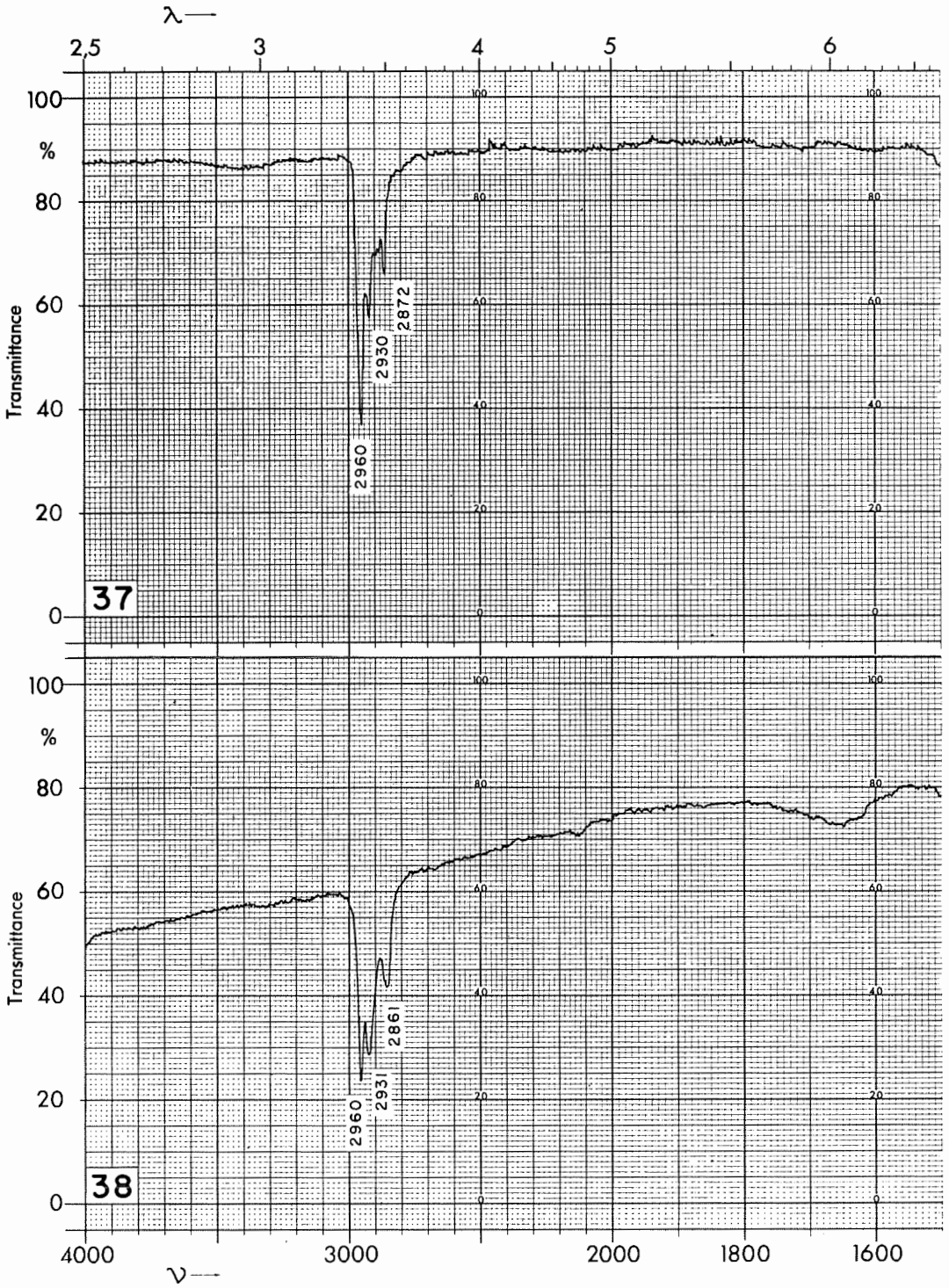

FIGURE 23. - Spectra of commercial flotation reagents (37) sodium isobutyl xanthate (AERO 317) and (38) potassium amyl xanthate (AERO 350).

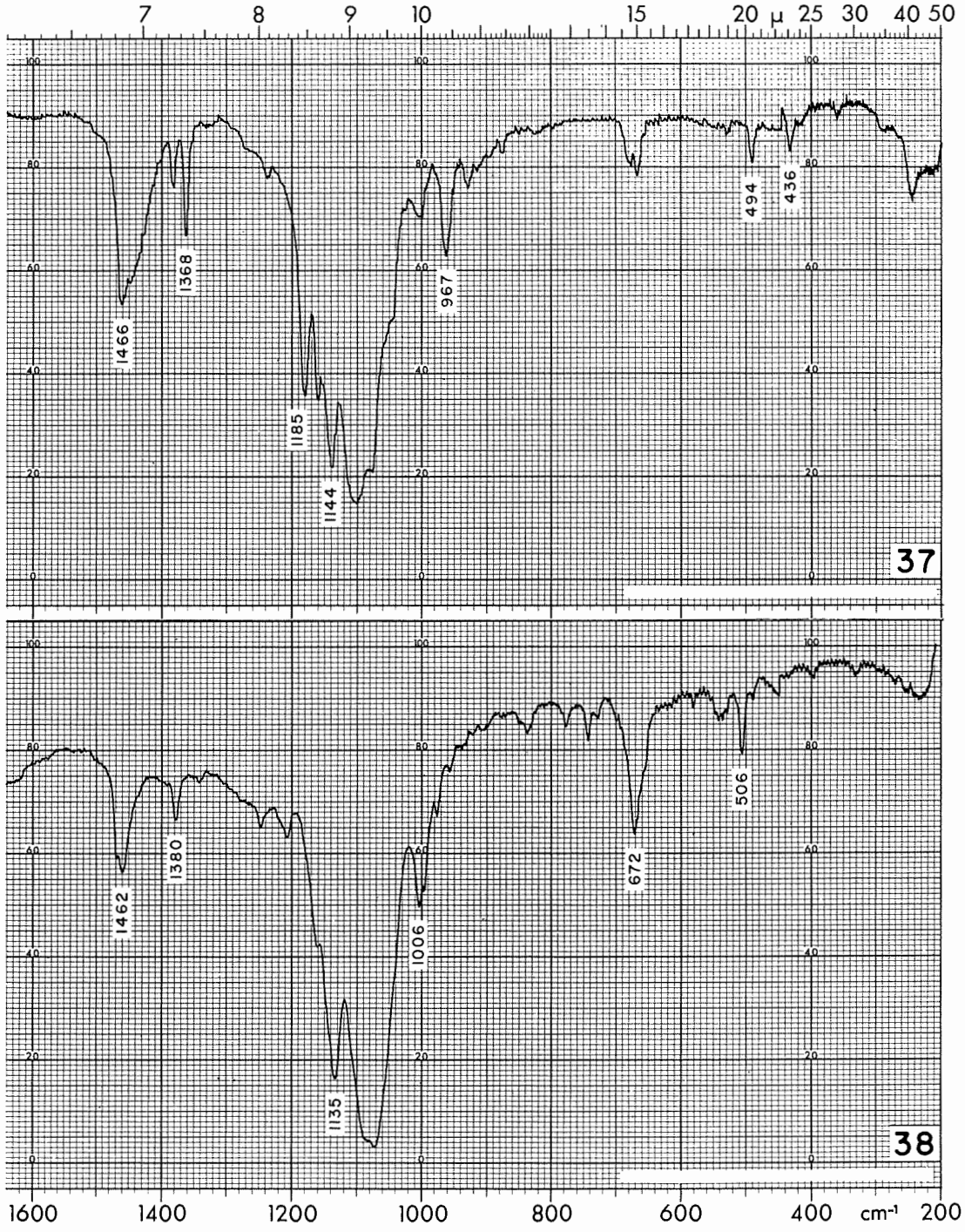

FIGURE 23. - Spectra of commercial flotation reagents (37) sodium isobutyl xanthate (AERO 317) and (38) potassium amyl xanthate (AERO 350).–Continued

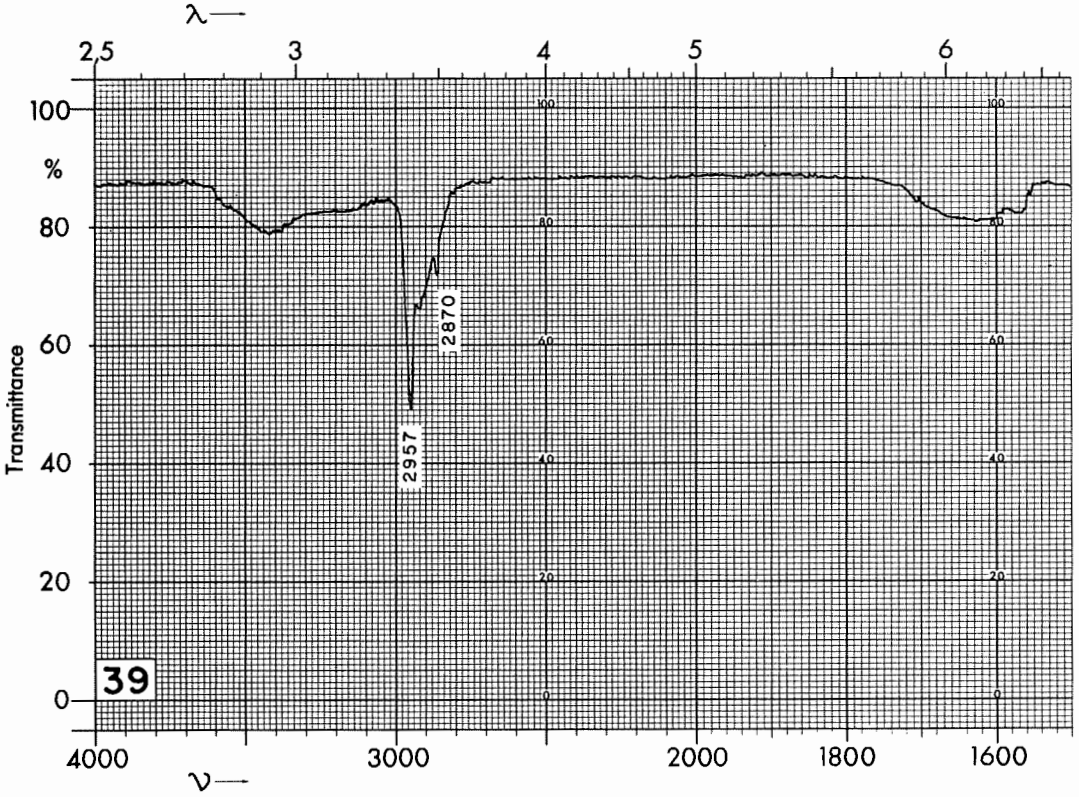

FIGURE 24. - Spectra of (39) commercial flotation reagent potassium hexyl xanthate (Dow Z-10).

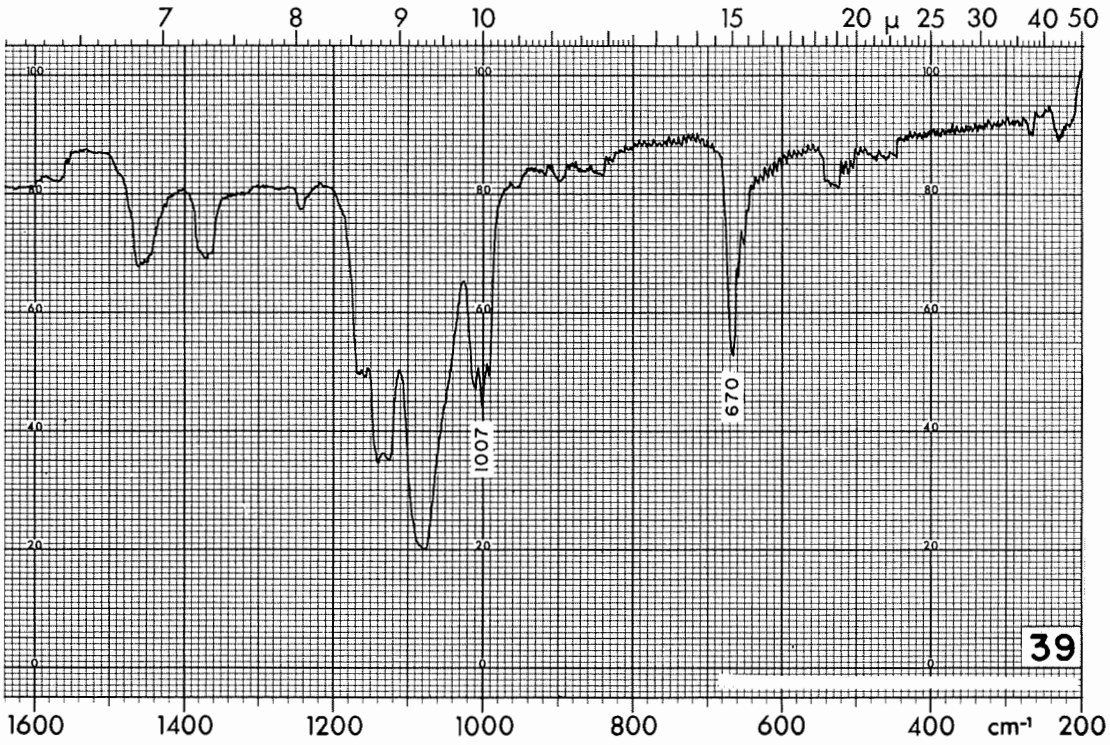

FIGURE 24. - Spectra of (39) commercial flotation reagent potassium hexyl xanthate (Dow Z-10).—Continued

REFERENCES

1. Allison, S. A., and N. P. Finkelstein. The Products of Reaction Between Galena and Aqueous Xanthate Solutions. Inst. of Min. and Met. (South Africa), Trans., v. 80, sec. C, December 1971, pp. C235-C239.

2. Allison, S. A., L. A. Goold, M. J. Nicol, and A. Granville. A Determination of the Products of Reaction Between Various Sulfide Minerals and Aqueous Xanthate Solution, and a Correlation of the Products With Electrode Rest Potentials. Met. Trans., v. 3, October 1972, pp. 2613-2618.

3. Coleman, R. E., and H. E. Powell. Infrared Spectroscopy Studies of a Xanthate-Galena System. BuMines RI 6816, 1966, 24 pp.

4. Coleman, R. E., H. E. Powell, and A. A. Cochran. Infrared Studies of Products of the Reaction Between Activated Zinc Sulfide and Potassium Ethyl Xanthate. Trans. Soc. Min. Eng., December 1967, pp. 408-412.

5. Goold, L. A., and N. P. Finkelstein. An Infrared Investigation of the Potassium Alkyl Xanthate and Alkyl Trimethyl Ammonium Bromide Mixed-Collector System. South Africa Nat. Inst. for Met., Res. Rept. 498, May 1969, pp. 12.

6. Greenler, R. G. An Infrared Investigation of Xanthate Adsorption by Lead Sulfide. J. Phys. Chem., v. 66, 1962, pp. 879-883.

7. Hunt, M. R., A. G. Krüger, L. Smith, and G. Winter. C-O, C-S, and M-S Vibration Frequencies of Metal Xanthates. Australian J. Chem., v. 24, 1971, pp. 53-57.

8. Leja, J., L. H. Little, and G. W. Poling. Xanthate Adsorption Studies Using Infra-Red Spectroscopy. 1.- Oxidized and Sulphidized Copper Substrates. 2.- Evaporated Lead Sulphide, Galena and Metallic Lead Substrates. Trans. Inst. Min. and Met., v. 72, 1963, pp. 407-423.

9. Little, L. H., G. W. Poling, and J. Leja. Infrared Spectra of Xanthate Compounds. II. Assignment of Vibrational Frequencies. Can. J. Chem., v. 39, 1961, pp. 745-754.

10. _____. Infrared Spectra of Xanthate Compounds. III. Organic Solvent Effect on the C = S Frequency. Can. J. Chem., v. 39, 1961, pp. 1783-1786.

11. Miller, R. G. J., ed. Laboratory Methods in Infrared Spectroscopy. Sadtler Res. Lab., Inc., Philadelphia Pa., p. 30.

12. Mukai, S., T. Wakamatsu, and M. Ichidate. Considerations on the Mechanism of Reaction Between Xanthate and Sulphide Minerals. Memoirs of the Faculty of Engineering. Kyoto Univ., v. 26, pt. 3, July 1964, pp. 195-207.

13. Pearson, F. G., and R. B. Stasiak. Infrared Spectra of Xanthates and Related Compounds. Appl. Spect., No. 4, 1958, pp. 116-120.

14. Plyer, E. K., and C. W. Peters. Wavelengths for Calibration of Prism Spectrometers. J. Res. Nat. Bur. Standards, v. 45, No. 6, December 1950, pp. 462-467.

15. Pure and Applied Chemistry. Tables of Wavenumbers for the Calibration of Infra-Red Spectrometers. V. 1, 1960, pp. 537-699.

16. Shankaranarayana, M. L., and C. C. Patel. Infrared absorption studies on some derivatives of xanthic, dithiocarbamic, and trithiocarbonic acids. Spectrochimica Acta, v. 21, 1965, pp. 95-103.

17. Szymanski, H. A. IR Theory and Practice of Infrared Spectroscopy. Plenum Press, New York, 1964, p. 55.

18. Takahashi, K., and I. Iwasaki. Inductive Effect of Polar Groups on Methyl Stretching Vibrations of Alkyl Groups and Its Implications in Flotation Chemistry. Trans. Soc. Min. Eng., AIME, v. 244, March 1969, pp. 66-71.

19. Yamasaki, T., and S. Usui. Infrared Studies of Xanthate Adsorbed on Zinc Sulfide. Trans. Soc. Min. Eng., March 1965, pp. 36-44.